The Lakes and Seas of Titan

Alexander G. Hayes

Department of Astronomy and Cornell Center for Astrophysics and Planetary Science, Cornell University, Ithaca, New York 14853; email: hayes@astro.cornell.edu

Annu. Rev. Earth Planet. Sci. 2016. 44:57–83

First published online as a Review in Advance on April 27, 2016

The *Annual Review of Earth and Planetary Sciences* is online at earth.annualreviews.org

This article's doi: 10.1146/annurev-earth-060115-012247

Keywords

Cassini, Saturn, icy satellites, hydrology, hydrocarbons, climate

Abstract

Analogous to Earth's water cycle, Titan's methane-based hydrologic cycle supports standing bodies of liquid and drives processes that result in common morphologic features including dunes, channels, lakes, and seas. Like lakes on Earth and early Mars, Titan's lakes and seas preserve a record of its climate and surface evolution. Unlike on Earth, the volume of liquid exposed on Titan's surface is only a small fraction of the atmospheric reservoir. The volume and bulk composition of the seas can constrain the age and nature of atmospheric methane, as well as its interaction with surface reservoirs. Similarly, the morphology of lacustrine basins chronicles the history of the polar landscape over multiple temporal and spatial scales. The distribution of trace species, such as noble gases and higher-order hydrocarbons and nitriles, can address Titan's origin and the potential for both prebiotic and biotic processes. Accordingly, Titan's lakes and seas represent a compelling target for exploration.

1. INTRODUCTION

SAR: Synthetic Aperture Radar

ISS: Imaging Science Subsystem

VIMS: Visual and Infrared Mapping Spectrometer

Saturn's largest moon, Titan, is the only extraterrestrial body known to support standing bodies of stable liquid on its surface and, along with Earth and early Mars, is one of three places in the Solar System known to have had an active hydrologic cycle. With an atmospheric pressure of 1.5 bar and surface temperature of 90–95 K, methane and ethane condense out of Titan's nitrogen-based atmosphere and flow as liquids on the surface (Lunine & Atreya 2008). On Titan, a methane-based hydrologic system produces surface features strikingly similar to terrestrial counterparts, including vast equatorial dune fields (Lorenz et al. 2006), well-organized channel networks that route material through erosional and depositional landscapes (Grotzinger et al. 2013), and lakes and seas filled with liquid hydrocarbons. These similarities make Titan a natural laboratory for studying the processes that shape terrestrial landscapes, probing extreme conditions impossible to recreate in earthbound laboratories.

Titan was discovered by Christiaan Huygens in 1655, but indications that it had an atmosphere did not come until telescopic observations of limb darkening by Comas Solá (1908); gaseous methane was identified in Titan's atmosphere by Kuiper (1944). The thickness and composition of Titan's atmosphere were determined by Lindal et al. (1983) using radio occultations of the 1980 *Voyager 1* flyby. Although *Voyager*'s optical instruments were unable to penetrate Titan's thick haze layers, the infrared spectrometer did detect hydrocarbons and nitriles in the stratosphere, confirming that methane and nitrogen were being converted into higher-order hydrocarbons and nitriles through the irreversible photochemical destruction of methane. In fact, Titan's surface liquids were originally predicted to be both a source and sink of methane photolysis (Lunine et al. 1983).

In order to penetrate Titan's thick atmosphere, the *Cassini* spacecraft was equipped with a K_u band ($\lambda = 2.16$ cm) Synthetic Aperture Radar (SAR) mapper capable of generating images at scales of ~300 m/pixel (Elachi et al. 2004). *Cassini*'s Imaging Science Subsystem (ISS) (Porco et al. 2004) and Visual and Infrared Mapping Spectrometer (VIMS) (Brown et al. 2003) have also observed Titan's surface through methane transmission windows. In one of its first observations, ISS revealed ~50 dark features poleward of 70°S. They were not initially referred to as lakes as they could not be reliably distinguished from dark equatorial dune fields (Porco et al. 2004). The first high-resolution SAR images of lakes were acquired in July 2006, when ~75 features with exceptionally low radar backscatter, high emissivity, and distinctly lacustrine morphologies were observed in the north polar region (Stofan et al. 2007). Subsequent observations have revealed more than 650 such features scattered through the polar regions (Hayes et al. 2008).

2. MORPHOLOGY AND DISTRIBUTION

Prior to *Cassini*'s arrival at Saturn, predicted features on Titan included crater lakes (Lorenz 1994), submerged impact craters (Lorenz 1997), cryovolcanic flows with pillow lava texture (Lorenz 1996), and an increased density of lacustrine features at polar latitudes (Lorenz & Lunine 1997). Although *Cassini* has not observed crater lakes or water-ammonia pillow lavas, it has confirmed that lacustrine features are restricted to polar latitudes, where colder temperatures and less volatile components lower the activity of methane and allow for persistent lakes and seas. Morphologically, Titan's polar landscape is dominated by rugged, topographically variable, and presumably ice-rich bedrock that has been overlain by organic-rich sedimentary deposits in the form of moderately dissected uplands and smooth undulating plains (**Figure 1**) (Birch et al. 2016a, Moore et al. 2014). The undulating plains are contained in elevated, potentially endorheic, basins that are topographically isolated by exposures of the dissected uplands and the underlying terrain (Birch

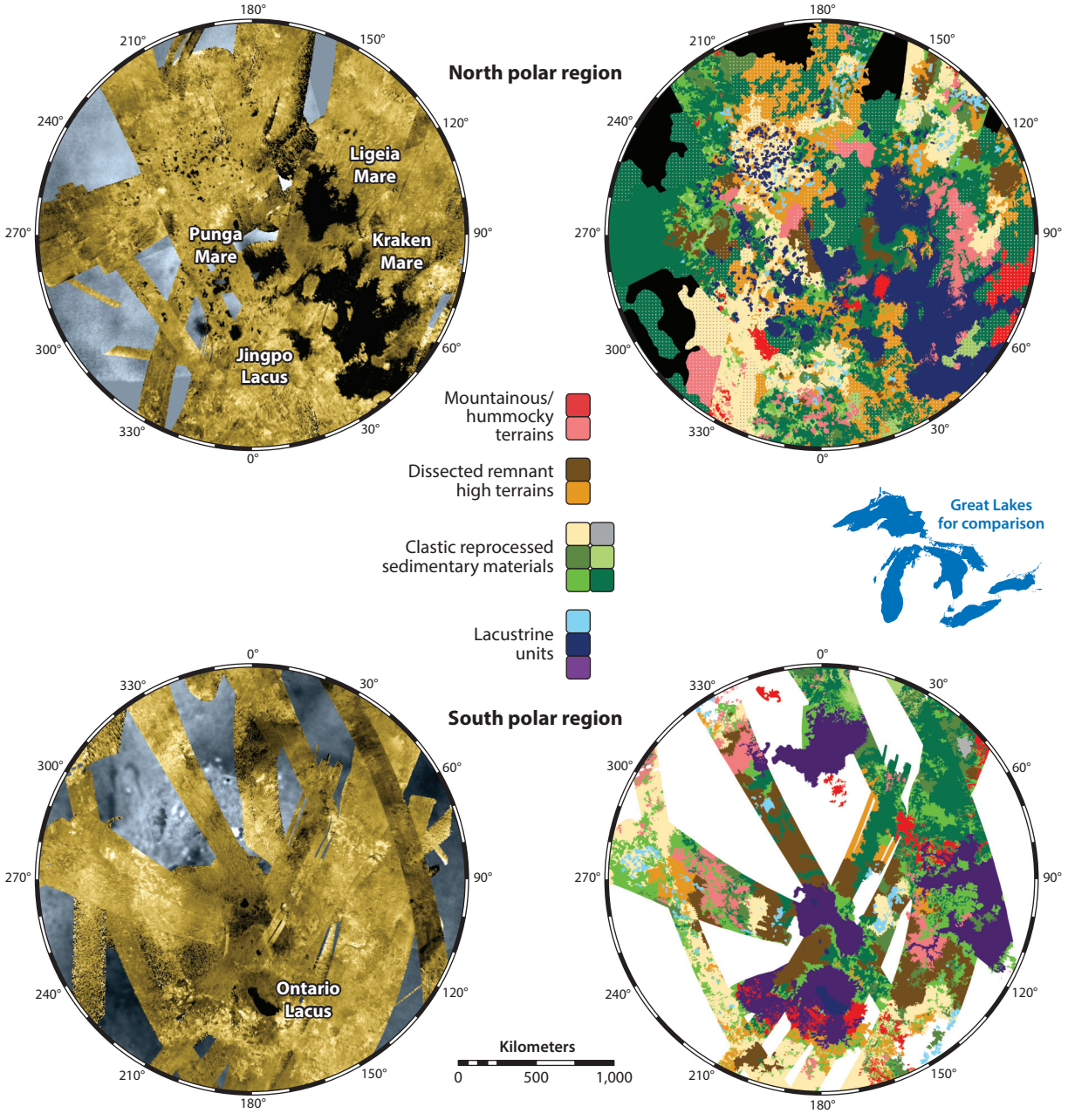

Figure 1

Polar distribution of hydrologic features on Titan derived from *Cassini* data acquired through January 2015 (flyby T108). The panels on the left depict false-color Synthetic Aperture Radar (SAR) mosaics (*gold*) overlying near-infrared Imaging Science Subsystem (ISS) maps (*gray*), with maria and lacūs identified. The panels on the right show the morphologic mapping units identified by Birch et al. (2016a). The relative topography of the mapped units is represented by the vertical arrangement of boxes in the central legend. Underlying terrain is mapped in red, the sedimentary undulating plains in orange, and the dissected uplands in various shades of green. Filled lakes and seas are shown in blue, whereas paleoseas and empty lake basins are shown in purple and cyan, respectively. An outline of Earth's Great Lakes in North America is included for scale.

et al. 2016a, Hayes et al. 2016a). Inset into these sedimentary deposits are broad and sharp-edged depressions (SEDs), which are found in varying states of liquid fill (dry, wet, and inundated) (Hayes et al. 2008, 2016b).

SED: sharp-edged depression

In the north, liquid-filled broad depressions make up the Kraken, Ligeia, and Punga Maria, as well as the larger lakes, including Jingpo and Bolsena Lacūs (**Figure 2**). In the south, dry broad depressions have been suggested to be paleoseas that were filled during an earlier epoch (**Figure 3**) (Aharonson et al. 2009, Hayes et al. 2011). Most of Titan's lakes are smaller SEDs that are morphologically distinct from the larger broad depressions (**Figure 4**). Over time, the material that composes the undulating plains and dissected uplands has been eroded and recycled, generating common morphologic units between the two poles that suggest similar formation pathways, although perhaps with variable initial conditions (Birch et al. 2016a, Hayes et al. 2008). In both polar regions, secondary erosional and depositional units have been identified, including alluvial fans (Birch et al. 2016b), deltas (Wall et al. 2010), fluvially reworked crenulated plains, and low-lying sedimentary material that contains large river valleys feeding into the maria (Burr et al. 2013).

Titan's seas, Kraken Mare (5.0×10^5 km^2), Ligeia Mare (1.3×10^5 km^2), and Punga Mare (6.1×10^4 km^2), represent 80% of all liquid-filled surfaces by area (Hayes et al. 2008). Altimetry measurements from the *Cassini* RADAR have shown that the liquid surfaces of all three maria are consistent with a single equipotential surface with a mean radius of ~2,574.1 km from Titan's center of mass, using the geoid reported by Iess et al. (2012). Altimetry shows that the surface elevations of Punga Mare and Kraken Mare are the same to within <8 m (1σ), limited by the delay resolution of RADAR's 10-MHz sampling bandwidth pointing accuracy (i.e., magnitude of off-nadir pointing) of the spacecraft. The surface elevation of Ligeia Mare, which was observed during a separate altimetry pass in May 2013 (flyby T104), is constrained to be within <50 m (1σ) of those of Punga and Kraken Maria, limited by the relative trajectory uncertainty between differing flybys. The similarity of the maria's liquid surface elevations suggests that they are hydraulically connected (Hayes et al. 2016a).

Altimetry measurements of three smaller, more distal lakes show liquid levels several hundred meters above the seas, suggesting that these lakes reside in isolated or perched drainage basins that may or may not be hydraulically connected to the maria. The elevations of empty basin floors were similarly observed to be above the maria in the north polar region, and Hayes et al. (2016a) found that they are regionally correlated (**Figure 5**). In the immediate vicinity of the maria, empty basin floor elevations never protrude below the maria's liquid elevation. In more distal topographic basins, basin floor elevations appear to lie above the elevation of the local liquid-filled lakes. These observations suggest that lake presence or absence is controlled by a phreatic surface (i.e., "groundwater" table) or local impermeable boundary within a given regional topographic basin. Whether or not the topographic basins are in communication remains unknown.

The diameters of Titan's lakes and seas follow a log-normal size distribution with a median of 77 ± 20 km (Hayes et al. 2008). The *Cassini* spacecraft has revealed 577 liquid-filled depressions that, excluding the three maria, cover a combined surface area of 2.13×10^5 km^2 across Titan's north and south polar regions. In addition, 295 putative empty lakes (dry SEDs) have been identified based on their morphology that cover a land area of 1.36×10^5 km^2. Finally, four putative paleomare basins have been found in the south polar region that cover 7.6×10^5 km^2 (Hayes et al. 2011, Birch et al. 2016a). Although the existence of modern equatorial and mid-latitude lakes has been proposed (Griffith et al. 2012, Vixie et al. 2015), and low-albedo candidates have been identified in lower-resolution VIMS observations, they have yet to be confirmed by higher-resolution radar imaging. Note, however, that transient ponding may occur following large-scale rain storms (Turtle et al. 2011a).

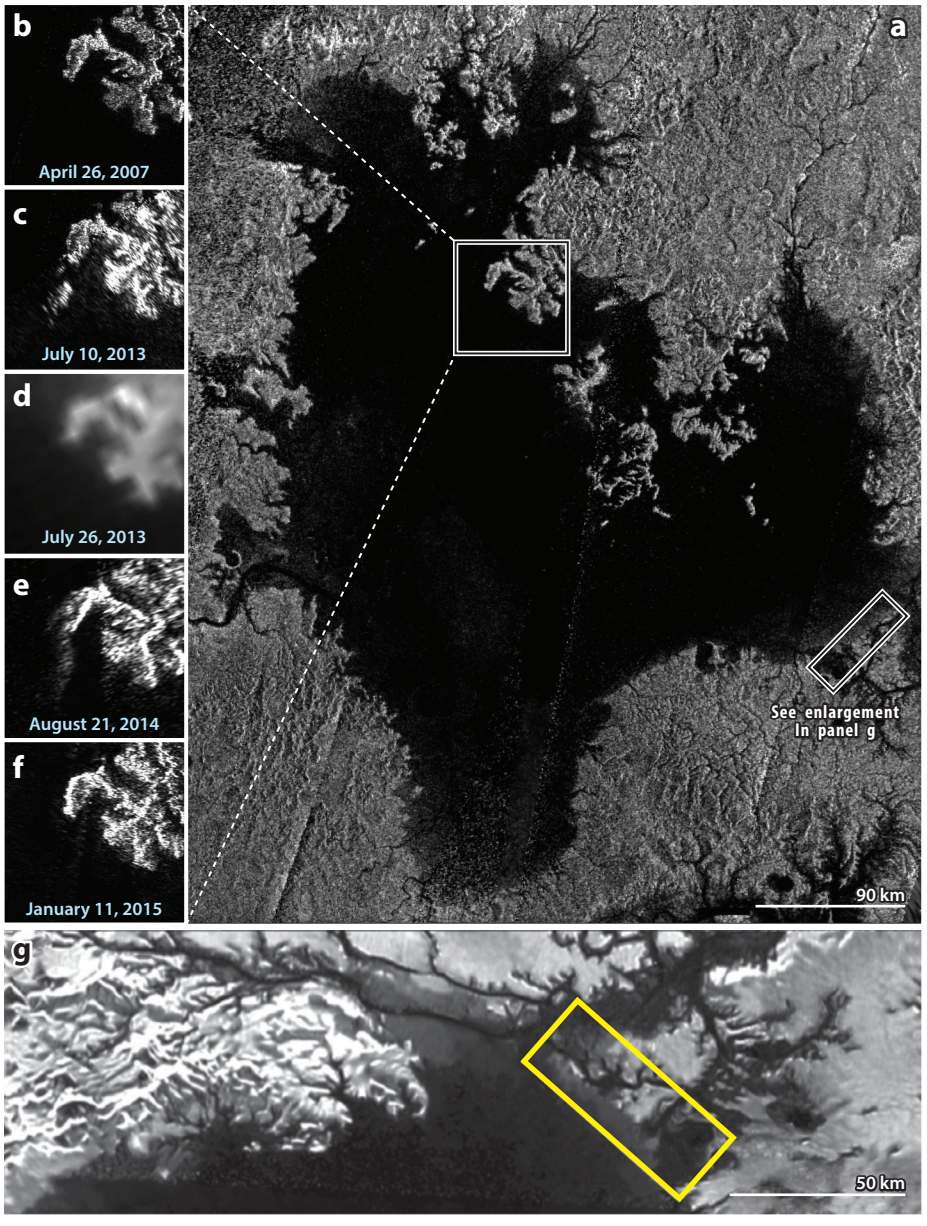

Figure 2

(*a*) Synthetic Aperture Radar (SAR) mosaic of Ligeia Mare, the second largest sea on Titan, assembled from data acquired between April 2007 and January 2015. Note the rough, crenulated shoreline and drowned river valleys near the top of the panel, suggesting the sea is flooding preexisting terrain. (*b–f*) A temporal sequence of the region surrounding Ligeia's magic island (Hofgartner et al. 2014). (*g*) A close-up of an area along the southeastern shore of Ligeia that has been despeckled using the algorithms described by Lucas et al. (2014). Note how the shoreline is encroaching on the preexisting drainage system and, in some cases, appears to be erasing topography in the terrain highlighted by the yellow box. Some pixels were modified to create new labels.

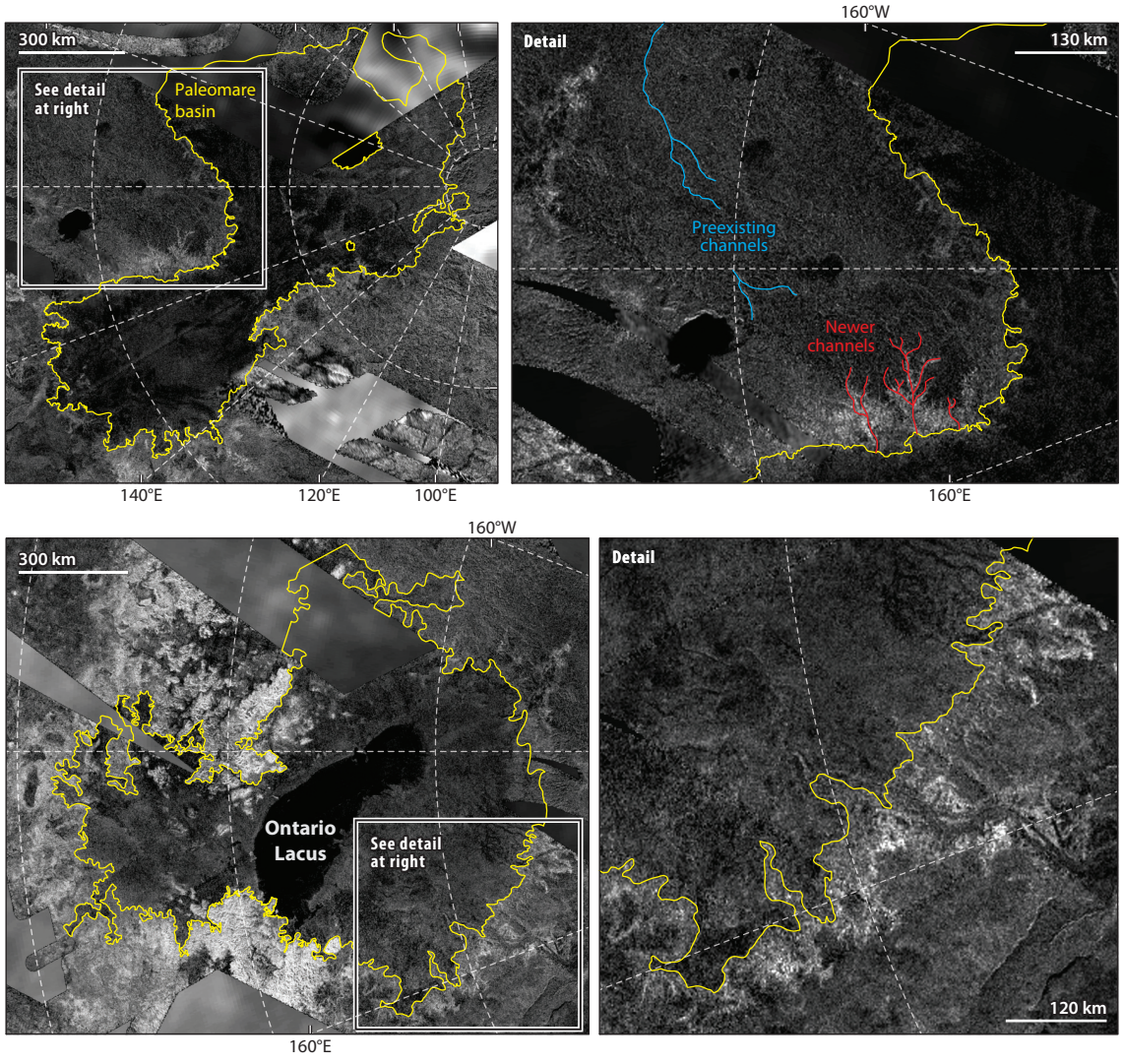

Figure 3

Synthetic Aperture Radar (SAR) mosaics showing examples of putative south polar paleomare basins (*left*), outlined in yellow. Details (*right*) show close-ups of the boxed regions. The top detail shows a close-up of the eastern shore of the basin depicted in the top mosaic, where a pulse of channel incision (channels mapped in red) appears to be eroding a recently exposed wall of the basin that is retreating into a preexisting plain, which appears (see channels mapped in blue) to be sloping in the opposite direction. This situation is consistent with response to a geologically recent reduction in base level, exposing the basin wall. The bottom detail shows a close-up of the western shoreline of the paleomare basin depicted in the bottom mosaic that contains Ontario Lacus.

In comparison, Earth has between 49 and 304 million active lakes and ponds, covering approximately 4×10^6 km^2 of land area (Downing et al. 2006, McDonald et al. 2012). However, only 1.8×10^5 terrestrial lakes have areas greater than the 1-km^2 detectability threshold of *Cassini* SAR. Fassett & Head (2008) conducted a global survey of Mars that identified 211 open paleolake systems with areas greater than 1 km^2. On all three bodies, the size-frequency distribution of moderate- to large-sized features (>100 km^2) follows a power law (**Figure 6**). This power law

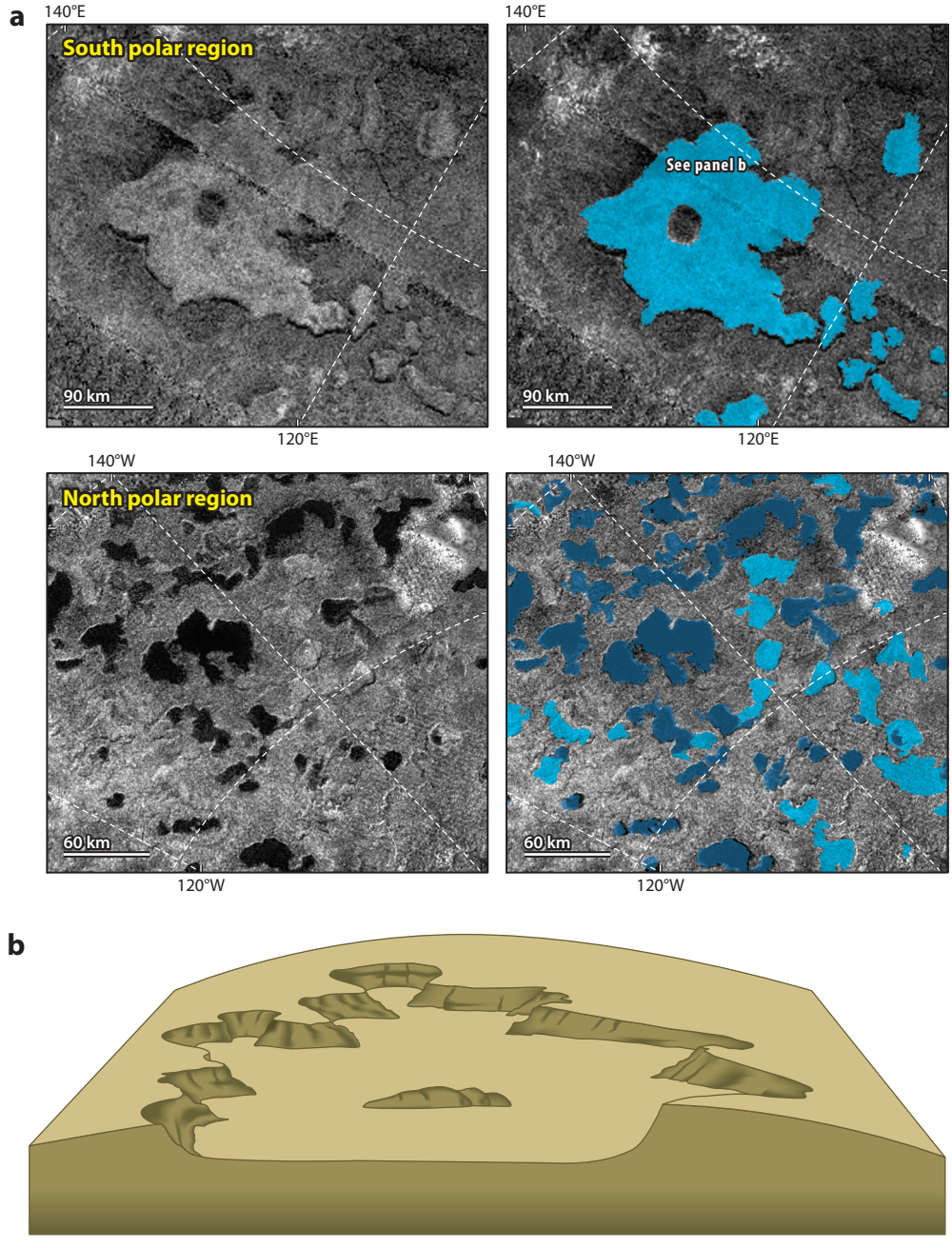

Figure 4

(*a*) Type examples of filled and empty sharp-edged depressions (SEDs) in the south (*top*) and north (*bottom*) polar regions. Lakes are depicted in dark blue and empty basins in cyan. Note the shape of the larger empty basins in the top images, which appears to be consistent with agglomeration of several smaller features. (*b*) An artist's depiction of the largest empty basin as viewed through a stereo display.

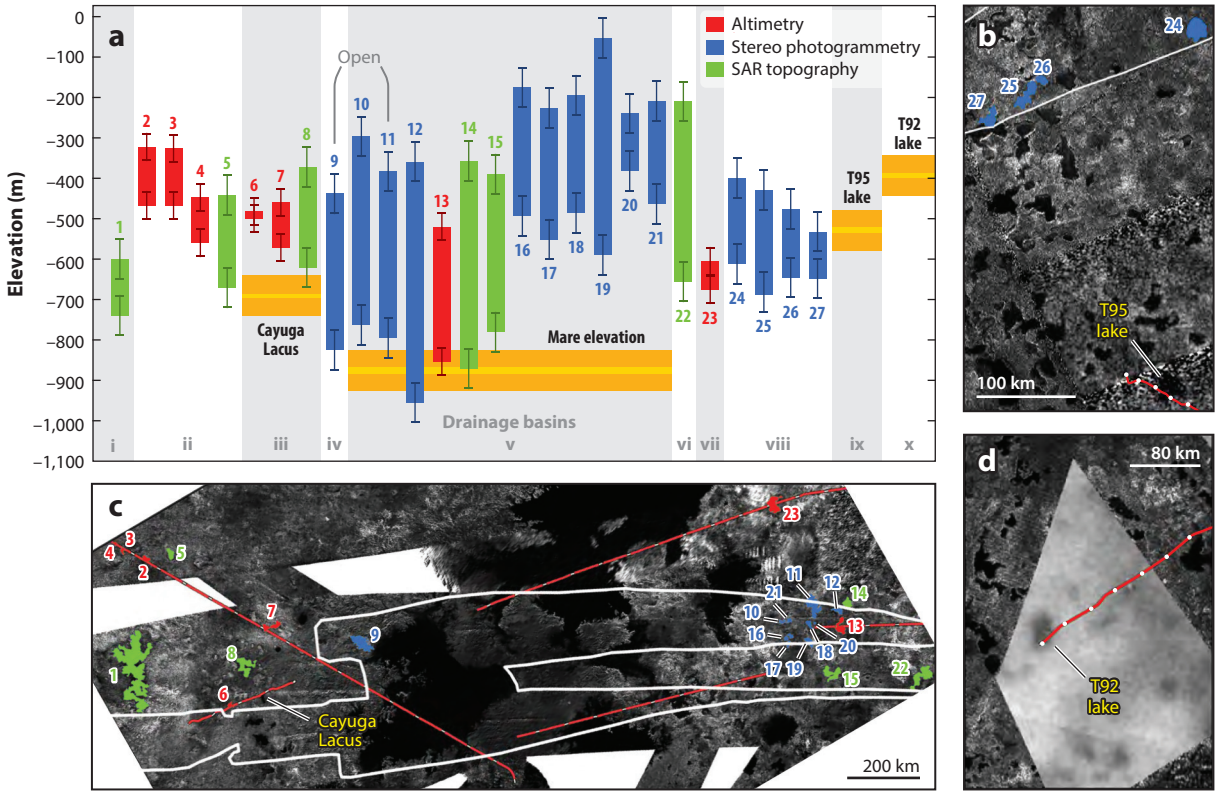

Figure 5

Elevation of empty basin floors relative to the liquid elevation of the mare and three smaller lakes. In the graph (panel *a*), the bottom of each bar represents the floor of an empty basin, and the top represents the height of the surrounding terrain. The different bar colors correspond to the different topographic sources [altimetry, stereo photogrammetry, and Synthetic Aperture Radar (SAR) topography]; the colors also correspond to the numbered features depicted in the three SAR mosaics (panels *b–d*). White outlines represent the extent of stereo photogrammetry coverage. To within error, none of the empty basin floors are observed to dip below the elevation of the mare shoreline.

relationship, which appears to be independent of basin formation processes (Sharma & Byrne 2011), highlights the fractal nature of each landscape (Hamilton et al. 1992). Compared to Earth, Mars and Titan have a dearth of small lakes relative to their cumulative totals (**Figure 5**). On Mars, this discrepancy has been attributed to preferential destruction of smaller features over the past 3.5 Gyr (Cabrol & Grin 2010). On Titan, an active hydrologic system suggests that differential erosion is unlikely to explain the departure from a power law. An alternative explanation is that there is a scale dependence to basin formation. Basins either initially form as large, kilometer-scale depressions or quickly grow to kilometer-scale sizes through processes such as scarp retreat following the generation of a smaller, seed basin.

Collectively, all liquid-filled depressions account for 1.1% of Titan's global surface area, similar to the 2.7% of Earth's land area covered by lakes and ponds (Hayes et al. 2008). Unlike Earth's lakes, Titan's lakes are predominantly located in the north, where they take up 12% of the area between 55°N and 90°N (as opposed to 0.3% of the area between 55°S and 90°S) (**Figure 1**). This dichotomy has been suggested to derive from Saturn's current orbital configuration, in which southern summer solstice is nearly coincident with perihelion and results in a 25% higher peak

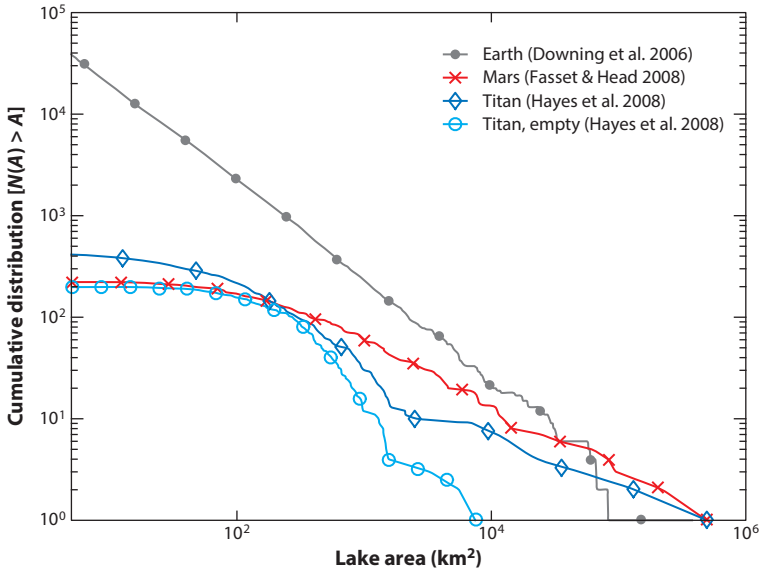

Figure 6

Size-frequency plots for lakes on Earth, Mars, and Titan. Source data were obtained from the references listed in the symbol key. Whereas Earth's lake frequencies are consistent with a simple power law model through all sizes, Mars and Titan exhibit a roll off for features smaller than $\sim 10^3$ km^2. On Mars, this has been attributed to differential erosion. On Titan, a more likely scenario is that basin formation mechanisms exhibit a size dependence.

solar flux than what is encountered during northern summer (Aharonson et al. 2009). Over many seasonal cycles, this flux asymmetry may lead to net transport of methane and ethane from the south to the north. As Saturn's orbital parameters shift due to apsidal precession and cyclic eccentricity variations, the net flux of northward-bound volatiles would presumably slow and eventually reverse. If this hypothesis is correct, the distribution of liquid deposits on Titan should oscillate between the poles, driven by a process analogous to Croll-Milankovitch cycles on Earth. Some general circulation models (GCMs) of Titan's climate have shown that the current asymmetric forcing is sufficient to drive methane and ethane to the north (Schneider et al. 2012) and that past and future orbital configurations could similarly drive liquid to the south over tens to hundreds of millennia (Lora et al. 2014). The dominant frequency, driven by Saturn's perihelion precession, is 45 kyr, but longer frequencies (e.g., 270 kyr) are also present.

The morphology of both dry and filled broad depressions presents a record of past and current climatic conditions. For example, Titan's northern maria have shorelines that include shallow bays with well-developed drowned river valleys (Stofan et al. 2007). These drowned valleys indicate that once well-drained upland landscapes became submerged as rising fluid levels outpaced sediment deposition. As the base level rose, the shores of the maria encroached upon the preexisting landscape and, in some cases, appear to have erased topography, as evidenced by the abrupt termini of large river valleys along the southeastern shore of Ligeia Mare (**Figure 2*g***) (Aharonson et al. 2014). In contrast, the largest southern lake, Ontario Lacus, expresses depositional morphologies along its western shoreline, which include lobate structures interpreted as abandoned deltas (**Figure 7**) (Cornet et al. 2012a, Wall et al. 2010). In the south, low-lying dark regions have been identified that may represent ancient maria that once encompassed areas comparable to their northern counterparts (Birch et al. 2016a, Hayes et al. 2011). Within these paleomaria there is

GCM: general circulation model

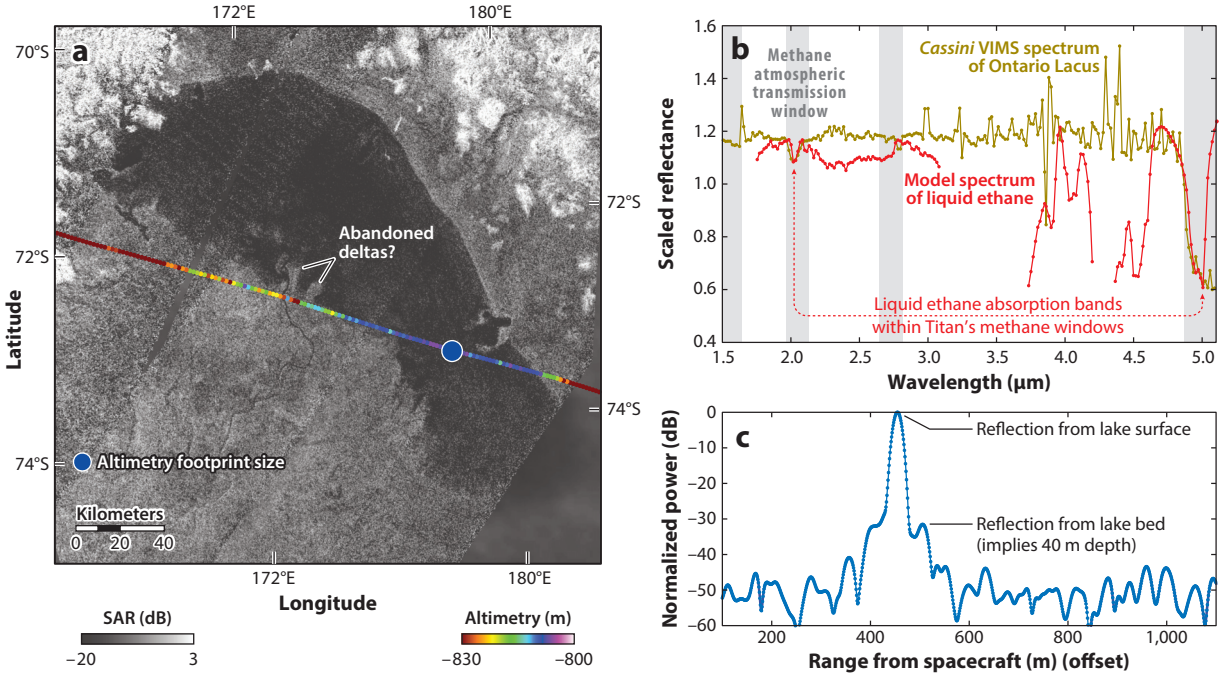

Figure 7

(*a*) Synthetic Aperture Radar (SAR) mosaic of Ontario Lacus, the largest filled lake in Titan's south polar region. The footprint locations of the December 2008 (flyby T49) altimetry pass are overplotted. Note the complex western shoreline and lobate features that have been interpreted as abandoned deltas, both of which have been used to suggest a long-term net reduction in liquid level. (*b*) A laboratory spectrum of liquid ethane in red (300-μm path length) and a Visual and Infrared Mapping Spectrometer (VIMS) spectrum of Ontario in dark yellow (relative to the shoreline reflectance). The gray bands depict the methane transmission windows. Note the agreement between the lab spectrum and observations at both 2 μm and 4.9 μm, which Brown et al. (2008) argue indicates the presence of liquid ethane. Panel *b* was generated using data from Brown et al. (2008). (*c*) A processed altimetry echo from the T49 observation, highlighting the secondary peak that comes from Ontario's lake bed.

evidence for channel incision (as a response to base level reduction) that has, in at least one location, propagated across what appears to be a preexisting and less dissected plain (**Figure 2*g***). These observations are consistent with a slow increase in base level in the north, at the expense of the south, for the past several tens of millennia.

At infrared wavelengths, Ontario Lacus possesses a series of margins, or bathtub rings, that are bright at 5 μm and have been interpreted as organic evaporites deposited along paleoshorelines (Barnes et al. 2009, Moriconi et al. 2010). Barnes et al. (2011a) identified similar 5-μm bright deposits in a subset of the northern SEDs and maria. MacKenzie et al. (2014) mapped the global distribution of these deposits and found that they cover ∼1% of Titan's surface. The largest exposures of the 5-μm bright deposits outside of the poles are found near the equator at Hotei and Tui Regiones, which have been interpreted as possible low-latitude paleoseas (Moore & Howard 2011). A lack of observed 5-μm bright evaporite deposits in the southern paleomare basins confounds their interpretation as paleoseas in the absence of an efficient removal or burial mechanism, as such deposits would be expected (MacKenzie et al. 2014).

Whereas Titan's larger lakes and seas appear to have developed in part through inundation of a preexisting well-drained landscape, the smaller liquid-filled SEDs appear to have originated

through different mechanisms. SEDs have relatively flat floors, significant depths (up to 600 m), and no apparent inflow or outflow channels at the resolution of the *Cassini* RADAR. These observations create a potential mass conservation problem, as basin formation requires significant removal of material from topographically closed depressions. The negative skewness in the curvature of SED planview boundaries is indicative of uniform scarp retreat (Howard 1990), and the complex form and stepwise floor topography of the largest SEDs are consistent with agglomeration of smaller retreating features (**Figure 3**) (Hayes et al. 2016a). To create the observed flat floors, retreat would have been coupled with the processes that remove excavated material. A subset of the SEDs (both filled and empty) also have hundred-meter-scale raised rims (Hayes et al. 2008, 2016a; Michaelides et al. 2016).

Taken together, these constraints challenge almost any basin formation model. The mechanisms that best fit the observations are sublimation or dissolution of a volatile substrate that underlies a more resistant cap layer, although it is unclear how to drive sublimation processes within Titan's poles (i.e., where are the cold traps, and what is the source material?). Subsurface fluid expulsion, similar to seafloor pockmark formation (Cathles et al. 2010) or mud volcanoes (Dimitrov 2002), may also work, but would require significant volumes of pressurized gas or liquid (perhaps N_2). Dissolution is compatible with uniform scarp retreat of a steep-sided depression that has no observable inflow or outflow channels, but it does not easily explain the raised rims. These features are not seen in traditional karst terrain (Ford & Williams 1989), although they may be explained by processes analogous to case-hardening (Williams 2008), pingo (Holmes et al. 1968), laccolith (Romanberdiel et al. 1995), or salt dome (Jackson et al. 1994) formation. Water ice is insoluble ($<10^{-11}$ mole fraction) in liquid hydrocarbons (Lorenz & Lunine 1996, Perron et al. 2006), requiring a significant fraction of the polar terrain to consist of soluble and/or volatile organic sediments (e.g., acetylene) with deposit thicknesses sufficient to accommodate SEDs with depths of up to 600–800 m (see **Figure 5**). Brown et al. (2006) suggested that the more volatile photolysis products, such as acetylene, could accumulate in polar cold traps over time, bringing more soluble material to the poles. Cornet et al. (2015) presented a karstic dissolution model for small lake formation on Titan; however, their model does not explain the presence of raised rims. Volcanic calderas have also been proposed (Wood et al. 2007), but these interpretations are handicapped by a lack of associated depositional features such as lava flows or cryoignimbrites. Regardless, a cryovolcanic origin could explain a minor subset of the smaller lakes that are characterized by circular depressions sitting atop topographic mounds (Wood 2015). Despite significant progress, understanding basin formation and evolution in Titan's polar regions remains an unanswered challenge. In particular, the SEDs are morphologically unique and may represent a key to understanding the formation and subsequent evolution of Titan's polar terrain.

3. BATHYMETRY

Despite prelaunch predictions that hydrocarbon liquids would be transparent to *Cassini*'s 13.8-GHz radar (Picardi et al. 1992a,b; Thompson & Squyres 1990) and that the RADAR's altimetry mode might be used as a sounder to probe Titan's liquids (Picardi et al. 1992b), experiments using liquefied natural gas by Paillou et al. (2008b) suggested that penetration depths would be significantly shallower than the altimetry mode's 35-m-range resolution (Elachi et al. 2004). Nevertheless, Mastrogiuseppe et al. (2014) successfully detected subsurface reflections in altimetry echoes acquired over Ligeia Mare in May 2013. The relatively low flyby altitude (1,600 km), combined with algorithmic suppression of the lateral lobes of the strong specular surface reflection, permitted the detection of reflections from the bottom of the sea (**Figure 8**). Along a 300-km track across Ligeia Mare, coherent processing of these echoes revealed the bottom

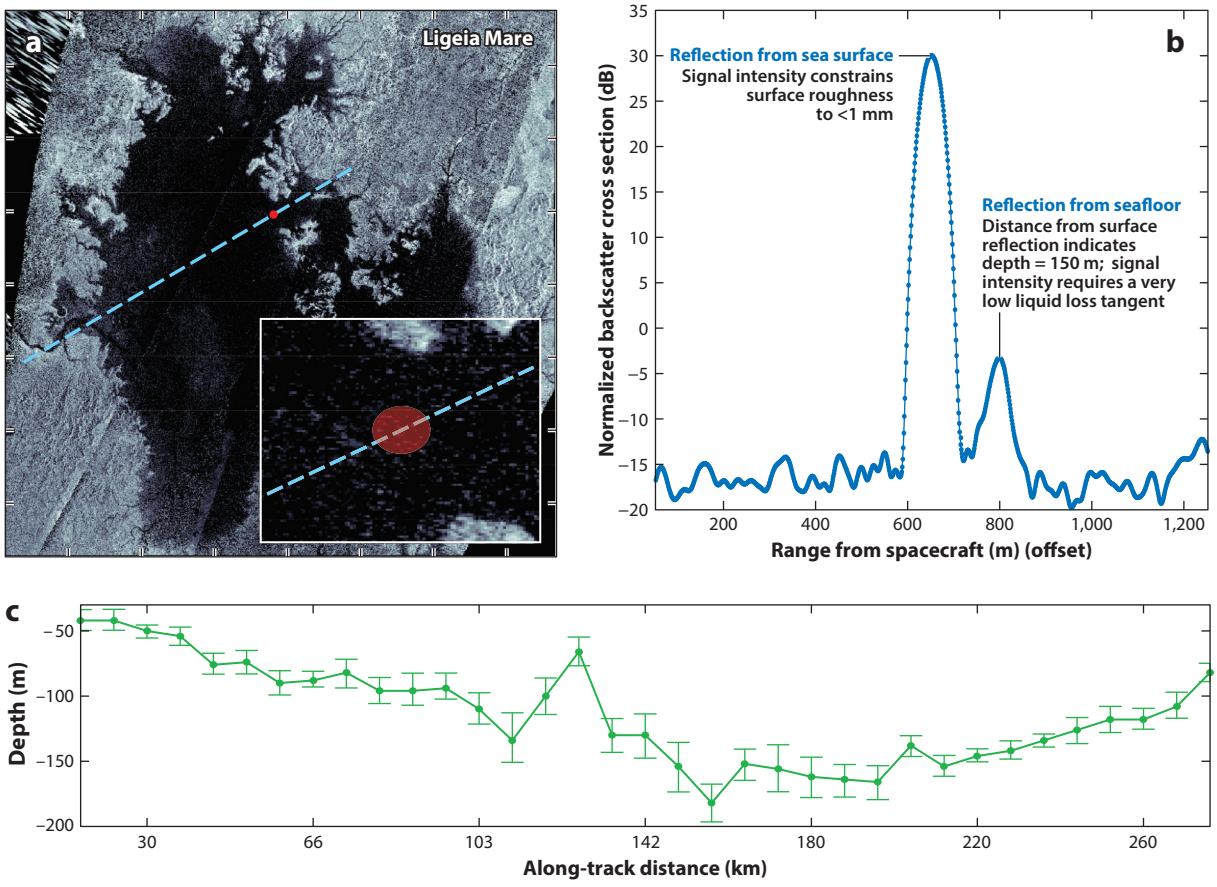

Figure 8

RADAR sounding measurements over Ligeia Mare. (*a*) A Synthetic Aperture Radar (SAR) mosaic of Ligeia Mare with the position of the May 2013 (flyby T91) altimetry track highlighted and the location of an example altimetry echo shown on the right. (*b*) An example of a double-peaked waveform observed over Ligeia, with returns from the sea surface and seabed labeled. (*c*) The along-track bathymetry derived by Mastrogiuseppe et al. (2014).

reflection and allowed construction of a bathymetry profile (**Figure 8*c***). The relative variations in received subsurface power as a function of depth provided an estimate for the liquid loss tangent $\tan \Delta = \varepsilon_i/\varepsilon_r = (4.35 \pm 0.85) \times 10^{-5}$ (Mastrogiuseppe et al. 2016b). The magnitude of the specular surface echo provided an upper limit on sea surface roughness of about 1 mm at the time of data acquisition (Zebker et al. 2014). Le Gall et al. (2016) calculated a similar loss tangent for Ligeia Mare using passive radiometry data, a technique originally proposed by Lorenz et al. (2003), obtained coincident with the active altimetry. Subsequent altimetry observations of Kraken and Punga Maria obtained in August 2014 and January 2015, respectively, also showed detectable subsurface echoes and suggested liquid absorptivities that are similar to that of Ligeia Mare. Portions of Kraken were too deep (or too absorptive) to detect subsurface returns (Mastrogiuseppe et al. 2016b). Recent laboratory experiments reported by Mitchell et al. (2015) confirmed the low microwave absorption of methane and ethane.

Mastrogiuseppe et al. (2016a) applied similar processing to low-altitude (∼1,800 km) altimetry acquired over Ontario Lacus in December 2008 and, despite significant saturation in many echoes,

detected subsurface reflections and retrieved depths of up to 50 m across the observed transect (**Figure 7**). These results are consistent with the near-shore depths reported by Hayes et al. (2010), which extended shoreline slopes into the lake. The loss tangent for Ontario derived by Mastrogiuseppe et al. (2016a) is $\tan \Delta = (7.0 \pm 3.0) \times 10^{-5}$. This is ~45% greater than the loss tangent reported for Ligeia Mare but an order of magnitude less than the absorptivity suggested by Hayes et al. (2010) from analysis of near-shore off-axis SAR. This discrepancy could be explained by an increase in microwave absorptivity near the shore resulting from an increased concentration of solutes or suspended particles as compared to the center of the lake. This is consistent with the observation that the near-shore ethane bands, unlike in central Ontario Lacus, are not saturated in VIMS (Brown et al. 2008). This suggests that photons are scattered before traveling through a path length sufficient to saturate the ethane absorption.

Prior to the work of Mastrogiuseppe et al. (2014), the unknown dielectric properties of both the liquid and the seabed limited the utility of SAR backscatter as a tool for estimating the depth of Titan's lakes and seas (Lorenz et al. 2010a, Notarnicola et al. 2009, Paillou et al. 2008a). With the bathymetry profile and liquid loss tangent of Ligeia Mare in hand, SAR data can be calibrated and used to generate bathymetric maps (**Figure 9*a***). Hayes et al. (2016b) derived an empirical backscatter function for the seabed using SAR backscatter in the altimetry footprints of Ligeia Mare. This empirical function was used to derive depths for all of the mare observations that have SAR returns above the instrument noise floor, assuming uniform seabed reflectivity. A similar analysis was performed for Ontario Lacus, revealing that the lake reaches depths of up to 90 m (**Figure 9*b***). Lorenz et al. (2014) calculated a liquid volume by assuming that sea depth was linearly

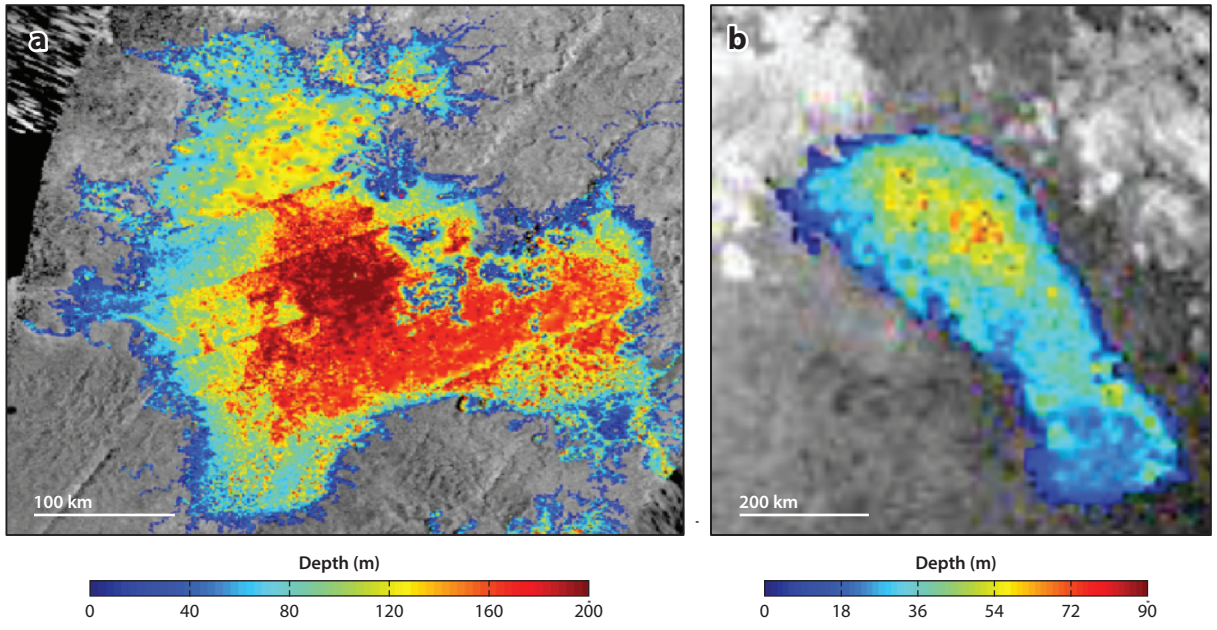

Figure 9

Synthetic Aperture Radar (SAR)-based bathymetric maps of (*a*) Ligeia Mare and (*b*) Ontario Lacus generated assuming a uniformly scattering seabed using the techniques and algorithms described by Hayes et al. (2016b). Ligeia Mare has an estimated volume of 14,000 km^3, equivalent to 2.8 times the volume of Earth's Lake Michigan. Ontario Lacus has an estimated volume of 560 km^3, equivalent to one-third the volume of Earth's Lake Ontario.

proportional to the distance from the nearest shoreline, calibrated such that the maximum depth of Ligeia Mare was 200 m and that the maximum depths of other maria scaled linearly with the square root of their area (Lorenz et al. 2008). Combining results from both techniques yields a lower limit of ~70,000 km^3 for the total volume of Titan's lakes and seas. If this liquid were spread across the surface equally it would be equivalent to a global ocean depth of ~1 m. This is equivalent to 14 times the volume of Lake Michigan, 300 times the mass of Earth's proven natural gas reserves, and 35 times the mass of all terrestrial fossil fuel reserves (natural gas, crude oil, and coal) (BP 2015). Unlike on Earth, where the total water content in the atmosphere (1.29×10^4 km^3) is only a fraction of the surficial reservoir (1.35×10^9 km^3), the moisture content in Titan's atmosphere is approximately seven times larger than the volume found in its lakes and seas. Unless Titan had a significantly larger liquid reservoir as compared to atmospheric methane, or currently has a large subsurface reservoir hidden from remote sensing, climate feedback would be improbable since the detectable volume is unlikely to significantly impact the atmospheric composition (McKay et al. 1993).

4. COMPOSITION

Before *Cassini* revealed the diverse nature of Titan's surface, Hunten (1973) suggested that there would be thick deposits of photochemical debris, and Lunine et al. (1983) calculated that prolonged methane photolysis would generate an ethane ocean with kilometer-scale depth. VIMS spectrally identified liquid ethane in Ontario Lacus (**Figure 7*b***) (Brown et al. 2008). Similar spectral identifications have been made in the northern seas and Jingpo Lacus. Due to ethane's high infrared absorption coefficients, the bands within the 2-μm methane window used to probe liquid ethane saturate after path lengths of only a few millimeters (Clark et al. 2010). As a result, the abundance of ethane in Ontario Lacus cannot be usefully constrained by VIMS. In order for VIMS to detect any signal in these bands (unsaturated absorption), either the lake needs to be a pond with millimeter-scale depth, which is inconsistent with the results of Mastrogiuseppe et al. (2014, 2016a), or there needs to be a layer of particulates in the top surface of Ontario that can scatter solar photons back toward the spacecraft.

Thermodynamic equilibrium models by Cordier et al. (2009, 2012) predicted ethane-rich lake compositions, whereas more recent work by Glein & Shock (2013) and Tan et al. (2013, 2015) predicted methane-dominated compositions at Titan's polar latitudes. Luspay-Kuti et al. (2015) attributed the differences between these models to the use of varying underlying theories relying on experimental data that may not be relevant in Titan conditions. The most recent experimental results reflect methane-dominated compositions. Using the laboratory measurements of Mitchell et al. (2015) and assuming a methane-ethane-nitrogen composition, Mastrogiuseppe et al. (2016b) determined that the measured best-fit loss tangent of Ligeia Mare was consistent with 71% CH_4, 12% C_2H_6, and 17% N_2 by volume, similar to the equilibrium compositions predicted by Glein & Shock (2013) and Tan et al. (2015). Note that if Titan's lakes are near vapor equilibrium with the atmosphere, evaporation rates should be significantly reduced despite their methane-dominated compositions.

Assuming a similar ternary composition, the increased best-fit loss tangent at Ontario Lacus is consistent with 49% CH_4, 41% C_2H_6, and 10% N_2 by volume. The higher loss tangent at Ontario could alternatively result from an increased abundance of more involatile hydrocarbons and/or nitriles; these species could be concentrated as a consequence of orbitally driven insolation cycles that may have slowly transported more volatile components (methane and ethane) to the north over the past several tens of millennia (Aharonson et al. 2009).

Nonpolar solutes such as acetylene (C_2H_2) and benzene (C_6H_6) may have low loss tangents similar to those of methane and ethane. Nitriles, such as hydrogen cyanide (HCN) and acetonitrile

(C_2H_3N), are likely quite absorptive, and even minor concentrations may affect the loss tangent. Once the complex permittivities of potential hydrocarbon and nitrile solutes in Titan's lakes are measured in the lab, they can be used to place upper limits on the concentration of these species in Titan's liquids. Regardless, the observed methane-dominated composition of the seas does not accommodate the inventory of ethane and other species suggested by photochemical models. This suggests that the products of methane photolysis fall into a sink other than the lakes and seas, such as crustal sequestration of ethane in clathrate hydrates (Choukroun et al. 2010, Mousis et al. 2014). Also of note is that, whereas the transparency of Ligeia Mare allows SAR backscatter to penetrate through over 100 m of liquid, the backscatter from many of the smaller lakes is below the radar's noise floor (Hayes et al. 2008). This suggests that these smaller lakes either are extremely deep or have a more absorptive composition than the seas do. The latter hypothesis is consistent with dissolution-based formation scenarios for the SEDs wherein liquids become saturated with soluble components from the regolith. Regardless, the lakes still cannot account for the missing ethane.

5. TIDES AND MIXING

On Titan, solar tides are negligible, but Saturn's gravity imparts a permanent tidal bulge of ~100 m at the sub- and anti-Saturnian points. Although Titan is tidally locked, its appreciable eccentricity ($e = 0.029$) leads to a 9% variation in tidal acceleration throughout each orbit (1 Titan day is 15.945 Earth days). This tidal forcing period is long enough such that even relatively shallow basins have natural periods that are too short to produce resonant effects (i.e., there is no Titan equivalent to the Bay of Fundy) (Lorenz 1994). Furthermore, Titan's seas, at least in modern times, are geographically limited, which limits their tidal variations.

Assuming a rigid crust, Tokano (2010) adapted the Bergen Ocean Model to Titan conditions and computed tidal amplitudes ranging from ~0.4 m for Ontario Lacus to ~5 m for Kraken Mare. Recent gravity measurements, however, have shown that Titan has a relatively large tidal Love number ($k_2 = 0.6$), implying the presence of a weak crust and a liquid water subsurface ocean (Iess et al. 2012). Titan's crust deforms with the semidiurnal tides, and the difference between the land and equipotential surface of its hydrocarbon seas is reduced by a factor of up to five, as compared to the earlier results of Tokano (2010) (Lorenz et al. 2014, Tokano 2010). Nevertheless, even these reduced tides can drive mixing among the northern seas and excite tidal currents of up to 0.2 cm/s (Tokano & Lorenz 2015). In fact, VIMS recently observed a broad and bright specular reflection across Trevize Fretum, Okahu Sinus, and Moray Sinus, which collectively encompass a channel system that connects Ligeia and Kraken Maria and has been interpreted as potential evidence for tidally driven flows between the seas (Sotin et al. 2015). Lorenz et al. (2014) noted that tidal currents can be locally magnified by constrictions such as straits and inlets (e.g., Seldom Fretum) and proposed that latitudinal variability in methane-rich precipitation can drive compositional gradients within Ligeia and Kraken that are seasonally stable. Compositional stability arises from the fact that tidal mixing may require between 5 and 70 Earth years to homogenize the basins.

Tokano & Lorenz (2015) investigated wind-driven circulation in Titan's seas and found that it is insignificant for much of the year but can become important from late spring through summer, when winds are predicted to freshen. According to their model, surface currents can become as high as 5 cm/s during the summer. This is large enough to affect the vertical structure of sea currents and form Ekman spirals (Tokano & Lorenz 2015). For weaker winds, however, Titan's slow rotation ensures that Coriolis effects are relatively minor.

Nontidal mixing mechanisms for Titan's lakes and seas include thermal overturning events and wind-driven circulation. Unlike water, which has a density maximum at 4°C, hydrocarbon liquids exhibit a monotonic decrease in density with increasing temperature. Thus, the mechanics

of thermal stratification in Titan's seas are simpler than for water bodies on Earth, but the potential for compositional layering is much more complex. Tokano (2005b, 2009a) examined the stability of Titan's seas and found that a stable surface layer of warm liquid could form during summer. Toward fall and winter, the surface would cool and potentially induce overturning events. Hydrocarbon solids are denser than their corresponding liquids, and in general, if ices should form (e.g., from evaporative cooling), they would sink and form deposits on the seafloor and thereby induce mixing (Tokano 2009b). It is important to note, however, that the presence of porosity and/or multicomponent liquid mixtures can allow floating solids for specific porosities and/or compositions (Hofgartner & Lunine 2013, Roe & Grundy 2012).

6. TEMPORAL VARIATIONS: WIND, WAVES, AND TRANSIENTS

On a local or regional level, there are three primary mechanisms by which a lake or sea can influence the climate: albedo effects, differences in heat capacity, and vapor or sensible heat exchange. On Earth, water's greater heat capacity, as compared to silicate-rich land, outweighs its low visible albedo and results in lakes that act as heat sinks to moderate local climates. The situation is not as clear on Titan. Tokano (2005a) used a GCM to show that the low albedo and thermal conductivity of liquid hydrocarbons can yield greater seasonal temperature variations (lower thermal inertia) than icy hydrocarbon surfaces. However, Tokano's work assumed a stagnant liquid. If tidal or wind-driven currents stir the lakes and seas, heat can be more effectively mixed, and the bulk thermal inertia of the lakes can be higher than that of the land, as it is on Earth. As a result, Titan's lakes can have either a positive or a negative effect on surrounding temperatures (Lorenz 2014).

Meteorological effects including fog (Brown et al. 2009b), lake-effect clouds (Brown et al. 2009a), and polar rainfall (Turtle et al. 2009) have been observed, suggesting that vapor is being introduced into the boundary layer by evaporation from the lakes and seas. Titan's ternary methane-ethane-nitrogen bulk liquid compositions allow for a wide range of evaporation rates because the saturation vapor pressure of ethane is orders of magnitude lower than that of methane. Similar to salt in water, the presence of both nitrogen and ethane lowers the activity of liquid methane and reduces evaporation rates, even allowing saturation, despite a lower relative humidity for pure methane and methane-nitrogen mixtures under the same conditions (Tan et al. 2013).

Whether or not Titan's seas can drive temperature gradients that enhance local winds, aeolian processes have clearly been active on Titan's surface, as evidenced by vast equatorial dune fields (Lorenz et al. 2006). The possibility of waves on Titan's lakes and seas was first described in detail by Srokosz et al. (1992) and inspired the installation of tilt sensors on the Huygens probe. Despite higher atmospheric pressure, lower gravity, and lower liquid surface tension (Lorenz et al. 2010b), *Cassini* has observed Titan's hydrocarbon lakes and seas to be remarkably calm for the majority of its mission, with vertical deviations of less than a few millimeters (Barnes et al. 2011b, Stephan et al. 2010, Wye et al. 2009, Zebker et al. 2014). One possibility is that polar winds are too weak to create waves; another possibility is that the seas may contain surface films or enough dissolved material to increase the viscosity and sufficiently damp waves. The latter hypothesis is difficult to reconcile with the low loss tangents observed by Mastrogiuseppe et al. (2014). The former requires detailed theoretical modeling to determine. Much of the parameterization for wind-wave models on Earth is empirical, despite laboratory studies that have demonstrated that wave growth depends on both gravity and fluid properties (Donelan & Plant 2009). As a result, Titan's exotic environment ensures that even rudimentary measurements of wave generation can provide valuable data to anchor physical models. Hayes et al. (2013) applied modern theories of wind-wave generation and propagation to Titan and concluded that the absence of wave activity observed during *Cassini*'s

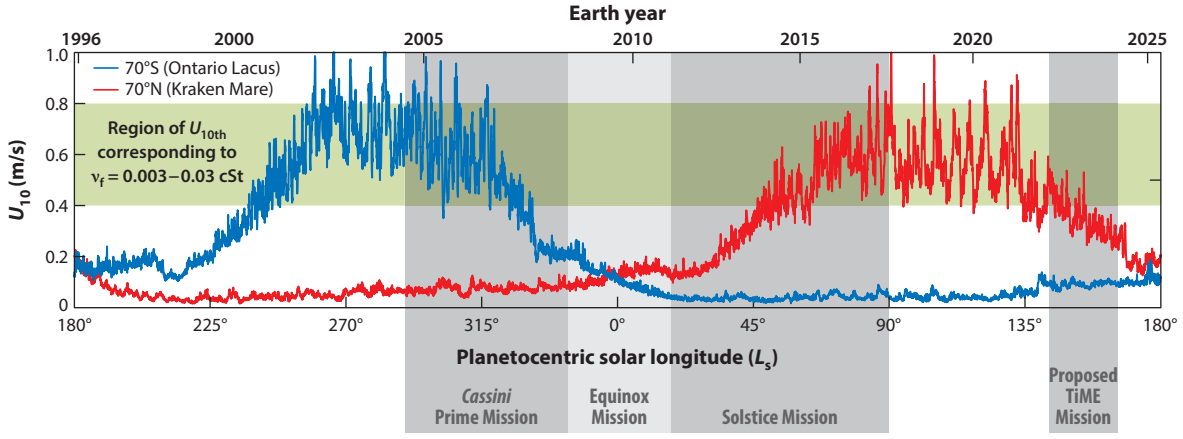

Figure 10

Wind speeds averaged over 24 h at 10 m (U_{10}) from Schneider et al. (2012) using a three-dimensional Titan general circulation model (GCM). Reported values represent the 95% quantile of the longitudinal wind distribution at 70°S and 70°N after averaging over five seasonal cycles. The green-shaded region highlights the expected range of threshold wind speeds (U_{10th}) for liquid viscosities (ν_f) ranging from pure methane (lower threshold) to pure ethane (upper threshold). Wind speeds are expected to exceed the threshold during the spring and summer but remain below even the minimum threshold during each pole's respective equinox and winter. The planetocentric solar longitude (L_s) ranges of the *Cassini* Prime, Equinox, and Solstice Missions and the proposed Titan Mare Exploration (TiME) Mission are shown at the bottom of the figure. Adapted with permission from figure 5 of Hayes et al. (2013).

Equinox Mission (June 2008 to December 2010) was likely a seasonal effect resulting from light winds during the winter and spring, and that the expected freshening of winds in northern summer (**Figure 10**) would be sufficient to cause sporadic ruffling of hydrocarbon sea surfaces.

Recently, *Cassini*'s previous series of nondetections have given way to indications of potential wave activity. Specifically, apparent sunglints offset from the geometric subsolar point have been observed in several of the lakes and seas (**Figure 11**) (Barnes et al. 2014), and transient bright radar signatures, known as Titan's magic islands, have been observed over the surfaces of Ligeia and Kraken Maria (**Figure 2*e*,*f***). The magic islands are a series of densely packed, anomalously reflective scatterers that originally appeared across an area 20 × 10 km in extent near Ligeia's northeastern shore. The most likely explanations for these features are bubbles, floating solids, or waves, which have been observed twice in Ligeia Mare over the course of six high-resolution observations acquired between February 2007 and January 2015 (Hofgartner et al. 2014, 2016).

Titan's low wind speeds are expected to produce significant wave heights of about 1 m only for the 2-m/s maximal winds predicted by most GCMs (Lorenz & Hayes 2012). These predicted waves are larger than expected tidal amplitudes and may be sufficient to cause shoreline erosion and produce coastal morphologies. Quantifying potential mechanisms of shoreline erosion (Kraal et al. 2006) remains an open research topic on Titan. When wind-waves are observed, their root mean square (RMS) surface heights, which can be measured by the RADAR (Wye et al. 2009) or calculated from the RMS slopes inferred from specular VIMS sunglints (Barnes et al. 2014), can be used to indirectly measure wind speeds via comparison with modeled wave fields. This effectively turns *Cassini* into an anemometer not dissimilar from many terrestrial radar systems (e.g., Brown et al. 1981).

In addition to waves and magic islands, other reported transient events have been interpreted to involve liquid evaporation and/or infiltration. Whereas there have been no definitive changes observed in the shorelines of the northern lakes and seas through January 2015 (flyby T108),

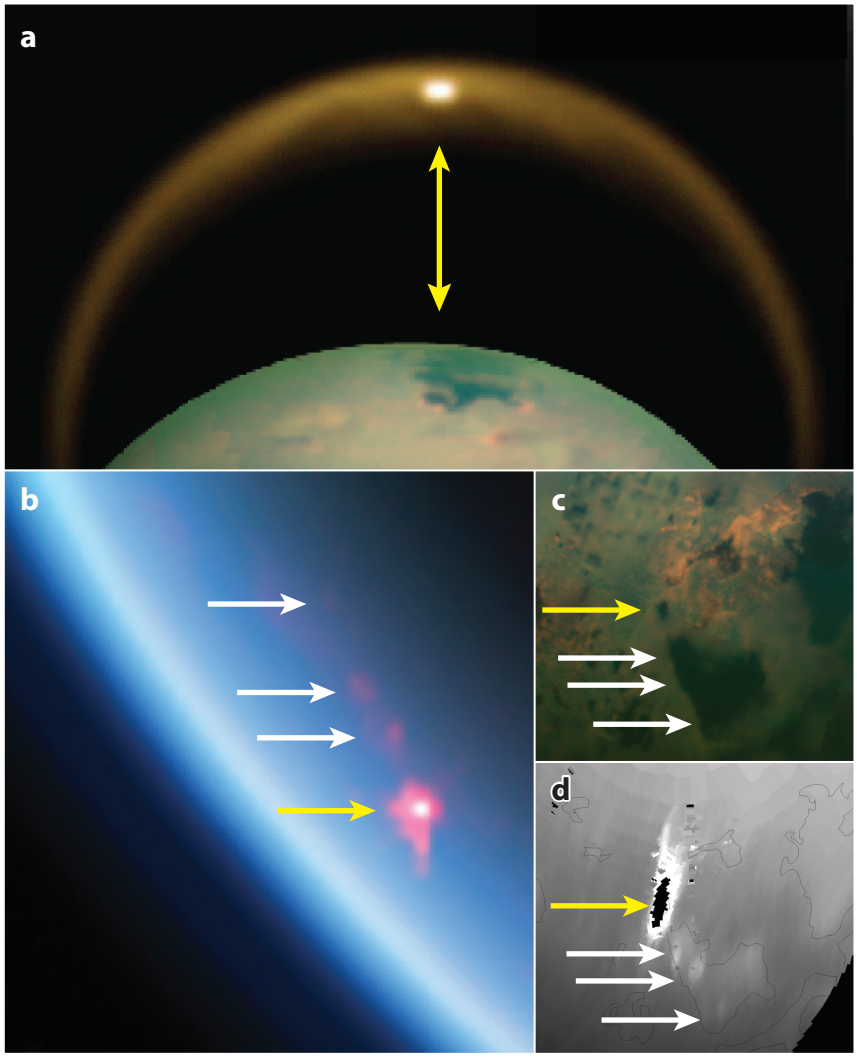

Figure 11

Visual and Infrared Mapping Spectrometer (VIMS) images of specular sunglints observed in (*a*) July 2009 (flyby T58), reported by Stephan et al. (2010), and (*b*) July 2012 (flyby T85), reported by Barnes et al. (2014). Whereas VIMS observed glints only at the subsolar point during flyby T58 (*yellow arrows*), requiring micrometer-smooth flat surfaces, several glints were observed at locations offset from the subsolar point during flyby T85 (*white arrows*). Barnes et al. (2014) argued that these spatially offset sunglints required roughness on the surface of Punga Mare, consistent with capillary-gravity wind-waves. An orthographic projection of January 2015 (flyby T108) VIMS observations of Kraken Mare is shown at the bottom of panel *a*, and orthographic projections of the T85 flyby are shown in panel *d* for context. Panel *a* is generated from NASA press release PIA12481, and panel *d* is adapted with permission from figure 1 (NASA PIA18433) and figure 4 of Barnes et al. (2014).

there have been several surface changes reported for lacustrine features in the south polar region. Specifically, Turtle et al. (2009, 2011b) discussed dark features that appeared in a topographic depression in the vicinity of Arrakis Planitia between ISS observations acquired in July 2004 and June 2005, shortly following southern summer solstice and bounding a large-scale south polar cloud system observed in October 2004. Turtle et al. (2011b) argued for shoreline recession at Ontario Lacus between June 2005 (Rev09, where Rev refers to an orbit of the *Cassini* spacecraft around Saturn) and March 2009 (flyby T51), although the poor resolution of T51 makes quantitative measures difficult. Cornet et al. (2012b) argued that, to within measurement error, the data are consistent with no changes at all. Hayes et al. (2011) discussed repeated RADAR passes of the south acquired in 2007 and 2008/2009 that contain lacustrine features that seem to disappear between subsequent SAR observations. The observed 10-fold increase in backscatter cannot easily be explained by geometric effects and suggests that, between the observations, liquid either infiltrated into the ground, evaporated, or did both (Hayes et al. 2011).

7. ASTROBIOLOGY

Titan has been identified as one of the most astrobiologically compelling targets in the Solar System (NRC 2011). In the current paradigm of our understanding of biological processes, it is likely that the formation and assembly of molecules into organized constructors and organelles of biologic systems necessitates a liquid solvent to allow said molecules to diffuse and interact (Pross & Pascal 2013). For life to originate, feedstock molecules created by chemistry through atmospheric, surface, or subsurface reactions must be dissolved, transported, and contained in liquid media. To determine where prebiotic organized chemistries and life could initiate and be maintained, we need to look in planetary environments that support liquids. Titan is the only known place, besides Earth, with both stable surface liquids and plentiful organics (Lunine & Atreya 2008). Furthermore, the greater cosmic abundance and lower luminosity of M dwarfs compared to solar analogs suggest that exoplanets with hydrocarbon-based hydrologic cycles may be more common than those with water-based hydrologic systems (Lunine 2010). Unlike the potential inhabitants of aqueous environments on Mars, Europa, or Enceladus or of Titan's own liquid-water interior ocean, any organisms that could thrive in Titan's lakes and seas would have a fundamentally alien biochemistry unlike that of any known terrestrial life (Bains 2004). Consequently, the search for biotic processes on Titan represents a test of life's cosmic ubiquity (Lunine 2009).

Despite an abundance of organic material (Raulin et al. 2009, 2012), biochemical processes on Titan must overcome significant challenges. Whereas terrestrial microorganisms are known to thrive on hydrocarbons in anaerobic conditions (Head et al. 2003), there are no known examples of terrestrial organisms that can live in nonaqueous media (Benner et al. 2004). The generally low solubility and relatively low available kinetic energy of the molecules in Titan's environment severely limit potential metabolic pathways (Malaska & Hodyss 2014). The hydrophobic nature of Titan's hydrocarbon cryosolvents requires different forms of cell compartmentalization, such as reverse micelles (Tung et al. 2008). Nevertheless, an apparent depletion of tropospheric molecular hydrogen (Strobel 2010) and the existence of surface acetylene deposits have inspired discussion of metabolisms based on methane (McKay & Smith 2005) and acetylene (Schulze-Makuch & Grinspoon 2005, 2006). Hörst et al. (2008) argued that oxygenated molecules, which can act as both reactants and catalysts for biologic processes, are delivered to Titan's atmosphere from the outgassing of geologic vents on Enceladus. If any biotic or prebiotic material exists in Enceladus's internal ocean (McKay et al. 2008), this too may be delivered to Titan. Although there are significant challenges and few insights regarding the nature of potential biochemistries on Titan (Benner 2004), their existence would revolutionize our understanding of the origin of life, which

makes Titan's lakes and seas essential destinations for future exploration (NASA 2014). Within the putative sedimentary deposits found around lake and sea shorelines, the strong gradient in volatility among hydrocarbon and nitrile species might lead to cycles of deposition and dissolution that concentrate products of the chemistry and mimic some of the prebiotic lacustrine processes that acted on Earth (Follmann & Brownson 2009) and possibly Mars (Farley et al. 2014).

8. FUTURE EXPLORATION

Just as Earth's history is tied to its oceans, Titan's origin and evolution are chronicled within the nature of its lakes and seas and their interactions with the atmosphere and surface. Although *Cassini* has provided a wealth of information regarding the distribution and morphology of liquid deposits on Titan, it has provided only the most basic information regarding their detailed composition, their role in Titan's volatile cycles, and their potential habitability. Addressing these fundamental topics, which link the lakes and seas to Titan's origin and evolution, requires visiting them in situ (Mitri et al. 2014). In situ exploration of Titan's lakes and seas would present an opportunity to understand the hydrocarbon cycle through their bulk liquid composition (methane, ethane, propane, etc.) (Lunine & Atreya 2008). It would provide a glimpse into the history of Titan's evolution as chronicled by noble gas abundance (argon, krypton, and xenon) (Owen & Niemann 2009) and isotopic composition (e.g., ^{12}C versus ^{13}C) (Niemann et al. 2010). It would allow an examination of trace organics (Raulin et al. 2009) in a natural laboratory for prebiotic chemistry and the limits of life. Meteorological and marine processes could be studied in an exotic environment that is drastically distinct from terrestrial experience (Lorenz 2014). A wide range of mission concepts have been proposed for Titan's future exploration (see Lorenz 2009 and Tobie et al. 2014 for recent summaries), including in situ exploration of its maria (Coustenis et al. 2009, Lorenz et al. 2015, Stofan et al. 2013). Study of the Titan Mare Exploration (TiME) concept (Stofan et al. 2013), for example, resulted in several engineering and mission design papers that will benefit future proposals (e.g., Lorenz 2015).

9. SUMMARY

The strange yet familiar nature of Titan's lakes and seas makes them one of the most scientifically compelling places in the Solar System. Despite material properties and environmental conditions vastly different from those on Earth, the source-to-sink sediment transport systems that sculpt polar landscapes generate strikingly consistent and familiar morphologic forms. Morphologies including abandoned deltas, paleomare basins, drowned river valleys, and embayed coastal features suggest a long-period cycling of liquid between Titan's poles as Saturn's orbital eccentricity and longitude of perihelion evolve. Whereas glacial and tectonic features are the dominant formation mechanisms for lacustrine basins on Earth, and impact cratering is the primary mechanism on Mars, the topographically closed, steep-sided, rimmed depressions that dominate Titan's lake basins suggest that dissolution processes are of primary importance on Titan. The detailed formation mechanisms responsible for generating these basins represent one of the keys to understanding the evolution of Titan's polar landscapes. Future efforts should focus on modeling their formation.

In contrast to the situation on Earth, where pole-to-pole oceans buffer the climate and contain a substantial mass of water relative to atmospheric reservoirs, Titan's lakes and seas are geographically isolated and represent only a small fraction of the methane content in the atmosphere. Although future observation and modeling campaigns are needed to elucidate the details of

specific lake-climate interactions, it appears that the bulk compositions of the seas are close to vapor equilibrium with the atmosphere and, contrary to pre-*Cassini* predictions, appear to be methane rather than ethane dominated. If methane has been present in Titan's atmosphere for a significant fraction of its history, as the landscape suggests, then there needs to be an unseen repository for the ethane generated by methane photolysis. Potential repositories include storage in subsurface liquid reservoirs and/or crustal clathrate hydrates. Regardless, the sheer volume of organic material required to generate the observed polar landscapes has yet to be reconciled with models of photolytic production.

As the Sun has begun to rise over Titan's north polar region during the *Cassini* Solstice Mission, the frequency of transient activity in the lakes and seas (e.g., waves and magic islands) has increased. It will be interesting to see whether this activity continues to grow as Titan approaches northern summer solstice. If it does, then the observations of transient features (e.g., wind-waves) can be used to constrain environmental parameters (e.g., wind speed) and help anchor physical models.

There is still much to learn about Titan's lakes and seas. In situ exploration will allow the determination of trace species, including the noble gas abundance and the mass distribution of higher-order hydrocarbons and nitriles; in situ data sets will provide information regarding the origin of Titan's atmosphere and help to test the limits of life by searching for signs of prebiotic and biotic processes. One must also recognize the massive public interest that the first extraterrestrial boat or submarine would garner in the community.

SUMMARY POINTS

1. Titan has a methane cycle analogous to Earth's water-based hydrologic cycle.
2. Liquid covers 1.1% of Titan's global area, similar to the 2.7% of Earth's land area covered by lakes and ponds.
3. The liquid elevations of Kraken, Ligeia, and Punga Maria are consistent with a single equipotential surface, suggesting that the seas are hydraulically connected.
4. Titan's maria have methane-dominated compositions that are apparently not the primary sink for the products of methane photolysis (e.g., ethane).
5. The collective volume of Titan's lakes and seas (~70,000 km^3) is one-seventh the volume of the atmospheric methane reservoir.
6. As the Sun rises in Titan's north polar region, transient events are being observed in the lakes and seas.
7. In Titan's lakes and seas—unlike in aqueous environments on Mars, Europa, and Enceladus—any organisms that could thrive would have a fundamentally alien biochemistry unlike that of any known terrestrial life.
8. Biochemical processes on Titan must overcome significant challenges, including low solubility and low available kinetic energy, which severely limit potential metabolic pathways.

DISCLOSURE STATEMENT

The author is not aware of any affiliations, memberships, funding, or financial holdings that might be perceived as affecting the objectivity of this review.

ACKNOWLEDGMENTS

I would like to thank Ralph Lorenz, Jonathan Lunine, Philip Nicholson, Steve Squyres, Jason Barnes, Melissa Brucker, Bryne Hadnott, and Alejandro Soto for detailed feedback and comments on this manuscript. I am also immensely grateful to Sam Birch, Jason Hofgartner, and Marco Mastrogiuseppe for assisting with several of the figures and providing feedback and comments on the text. Finally, I would like to sincerely thank the attendees of the Lakefest2015! workshop at Cornell University, who provided feedback and comments on an early version of this review. While writing this manuscript, I was partially supported by NASA *Cassini* Data Analysis Program grant NNX13AG03G.

LITERATURE CITED

Aharonson O, Hayes AG, Hayne PO, Lopes RM, Lucas A, Perron JT. 2014. Titan's surface geology. In *Titan: Interior, Surface, Atmosphere, and Space Environment*, ed. I Müller-Wodarg, CA Griffith, E Lellouch, TE Cravens, pp. 63–101. Cambridge, UK: Cambridge Univ. Press

Aharonson O, Hayes AG, Lunine JI, Lorenz RD, Allison MD, Elachi C. 2009. An asymmetric distribution of lakes on Titan as a possible consequence of orbital forcing. *Nat. Geosci.* 2:851–54

Bains W. 2004. Many chemistries could be used to build living systems. *Astrobiology* 4:137–67

Barnes JW, Bow J, Schwartz J, Brown RH, Soderblom JM, et al. 2011a. Organic sedimentary deposits in Titan's dry lakebeds: probable evaporite. *Icarus* 216:136–40

Barnes JW, Brown RH, Soderblom JM, Soderblom LA, Jaumann R, et al. 2009. Shoreline features of Titan's Ontario Lacus from *Cassini*/VIMS observations. *Icarus* 201:217–25

Barnes JW, Soderblom JM, Brown RH, Soderblom LA, Stephan K, et al. 2011b. Wave constraints for Titan's Jingpo Lacus and Kraken Mare from VIMS specular reflection lightcurves. *Icarus* 211:722–31

Barnes JW, Sotin C, Soderblom JM, Brown RH, Hayes AG, et al. 2014. *Cassini*/VIMS observes rough surfaces on Titan's Punga Mare in specular reflection. *Planet. Sci.* 3:1–17

Benner SA. 2004. Organic chemistry and the potential for life in the solar system. *Abstr. Pap. Am. Chem. Soc.* 228:U692

Benner SA, Ricardo A, Carrigan MA. 2004. Is there a common chemical model for life in the universe? *Curr. Opin. Chem. Biol.* 8:672–89

Birch SPD, Hayes AG, Dietrich WE, Moore J, Mastrogiuseppe M, et al. 2016a. Geomorphology of Titan's polar terrains: using landscape form to understand surface processes. *Icarus.* Submitted

Birch SPD, Hayes AG, Howard AD, Moore JM, Radebaugh J. 2016b. Alluvial fan morphology, distribution and formation on Titan. *Icarus* 270:238–47

BP. 2015. *BP Statistical Review of World Energy 2015.* London: BP. **http://www.bp.com/content/dam/bp/pdf/energy-economics/statistical-review-2015/bp-statistical-review-of-world-energy-2015-full-report.pdf**

Brown GS, Stanley HR, Roy NA. 1981. The wind-speed measurement capability of spaceborne radar altimeters. *IEEE J. Ocean. Eng.* 6:59–63

Brown ME, Schaller EL, Roe HG, Chen C, Roberts J, et al. 2009a. Discovery of lake-effect clouds on Titan. *Geophys. Res. Lett.* 36:L01103

Brown ME, Smith AL, Chen C, Adamkovics M. 2009b. Discovery of fog at the south pole of Titan. *Astrophys. J. Lett.* 706:L110

Brown RH, Baines KH, Bellucci G, Bibring JP, Buratti BJ, et al. 2003. Observations with the Visual and Infrared Mapping Spectrometer (VIMS) during Cassini's flyby of Jupiter. *Icarus* 164:461–70

Brown RH, Griffith CA, Lunine JI, Barnes JW. 2006. *Polar caps on Titan?* Presented at Eur. Planet. Sci. Congr., Berlin, Sept. 18–22. Abstr. 602

Brown RH, Soderblom LA, Soderblom JM, Clark RN, Jaumann R, et al. 2008. The identification of liquid ethane in Titan's Ontario Lacus. *Nature* 454:607–10

Burr DM, Perron JT, Lamb MP, Irwin RP, Collins GC, et al. 2013. Fluvial features on Titan: insights from morphology and modeling. *Geol. Soc. Am. Bull.* 125:299–321

Cabrol NA, Grin EA. 2010. Searching for lakes on Mars: four decades of exploration. In *Lakes on Mars*, ed. NA Cabrol, EA Grin, pp. 1–29. Amsterdam: Elsevier
Cathles LM, Su Z, Chen DF. 2010. The physics of gas chimney and pockmark formation, with implications for assessment of seafloor hazards and gas sequestration. *Mar. Pet. Geol.* 27:82–91
Choukroun M, Grasset O, Tobie G, Sotin C. 2010. Stability of methane clathrate hydrates under pressure: influence on outgassing processes of methane on Titan. *Icarus* 205:581–93
Clark RN, Curchin JM, Barnes JW, Jaumann R, Soderblom L, et al. 2010. Detection and mapping of hydrocarbon deposits on Titan. *J. Geophys. Res.* 115:E10005
Comas Solá J. 1908. Observations des satellites principaux de Jupiter et de Titan. *Astron. Nachr.* 179:289
Cordier D, Mousis O, Lunine JI, Lavvas P, Vuitton V. 2009. An estimate of the chemical composition of Titan's lakes. *Astrophys. J. Lett.* 707:L128–31
Cordier D, Mousis O, Lunine JI, Lebonnois S, Rannou P, et al. 2012. Titan's lakes chemical composition: sources of uncertainties and variability. *Planet. Space Sci.* 61:99–107
Cornet T, Bourgeois O, Le Mouelic S, Rodriguez S, Gonzalez TL, et al. 2012a. Geomorphological significance of Ontario Lacus on Titan: integrated interpretation of Cassini VIMS, ISS and RADAR data and comparison with the Etosha Pan (Namibia). *Icarus* 218:788–806
Cornet T, Bourgeois O, Le Mouelic S, Rodriguez S, Sotin C, et al. 2012b. Edge detection applied to Cassini images reveals no measurable displacement of Ontario Lacus' margin between 2005 and 2010. *J. Geophys. Res.* 117:E07005
Cornet T, Cordier D, Le Bahers T, Bourgeois O, Fleurant C, et al. 2015. Dissolution on Titan and on Earth: toward the age of Titan's karstic landscapes. *J. Geophys. Res. Planets* 120:1044–74
Coustenis A, Lunine J, Lebreton JP, Matson D, Erd C, et al. 2009. Earth-based support for the Titan Saturn System Mission. *Earth Moon Planets* 105:135–42
Dimitrov LI. 2002. Mud volcanoes—the most important pathway for degassing deeply buried sediments. *Earth-Sci. Rev.* 59:49–76
Donelan MA, Plant WJ. 2009. A threshold for wind-wave growth. *J. Geophys. Res.* 114:C07012
Downing JA, Prairie YT, Cole JJ, Duarte CM, Tranvik LJ, et al. 2006. The global abundance and size distribution of lakes, ponds, and impoundments. *Limnol. Oceanogr.* 51:2388–97
Elachi C, Allison MD, Borgarelli L, Encrenaz P, Im E, et al. 2004. RADAR: the Cassini Titan radar mapper. *Space Sci. Rev.* 115:71–110
Farley KA, Malespin C, Mahaffy P, Grotzinger JP, Vasconcelos PM, et al. 2014. In situ radiometric and exposure age dating of the martian surface. *Science* 343:1247166
Fassett CI, Head JW. 2008. Valley network-fed, open-basin lakes on Mars: distribution and implications for Noachian surface and subsurface hydrology. *Icarus* 198:37–56
Follmann H, Brownson C. 2009. Darwin's warm little pond revisited: from molecules to the origin of life. *Naturwissenschaften* 96:1265–92
Ford DC, Williams PW. 1989. *Karst Geomorphology and Hydrology*. London: Unwin Hyman
Glein CR, Shock EL. 2013. A geochemical model of non-ideal solutions in the methane-ethane-propane-nitrogen-acetylene system on Titan. *Geochim. Cosmochim. Acta* 115:217–40
Griffith CA, Lora JM, Turner J, Penteado PF, Brown RH, et al. 2012. Possible tropical lakes on Titan from observations of dark terrain. *Nature* 486:237–39
Grotzinger JP, Hayes AG, Lamb MP, McLennan SM. 2013. Sedimentary processes on Earth, Mars, Titan, and Venus. In *Comparative Climatology of Terrestrial Planets*, ed. SJ Mackwell, AA Simon-Miller, JW Harder, MA Bullock, pp. 439–72. Tucson: Univ. Ariz. Press
Hamilton SK, Melack JM, Goodchild MF, Lewis W. 1992. Estimation of the fractal dimension of terrain from lake size distributions. In *Lowland Floodplain Rivers: Geomorphological Perspectives*, ed. PA Carling, GE Petts, pp. 145–63. Chichester, UK: Wiley
Hayes A, Aharonson O, Callahan P, Elachi C, Gim Y, et al. 2008. Hydrocarbon lakes on Titan: distribution and interaction with a porous regolith. *Geophys. Res. Lett.* 35:L09204
Hayes AG, Aharonson O, Lunine JI, Kirk RL, Zebker HA, et al. 2011. Transient surface liquid in Titan's polar regions from Cassini. *Icarus* 211:655–71
Hayes AG, Birch SPD, Dietrich WE, Howard AD, Kirk R, et al. 2016a. Topographic constraints on the evolution and connectivity of Titan's lacustrine basins. *Geophys. Res. Lett.* Submitted

Hayes AG, Birch SPD, Michaelides RJ, Hofgartner JD, Loren RD, et al. 2016b. The distribution and volume of Titan's hydrocarbon lakes and seas. *Nat. Geosci.* Submitted
Hayes AG, Lorenz RD, Donelan MA, Manga M, Lunine JI, et al. 2013. Wind driven capillary-gravity waves on Titan's lakes: hard to detect or non-existent? *Icarus* 225:403–12
Hayes AG, Wolf AS, Aharonson O, Zebker H, Lorenz R, et al. 2010. Bathymetry and absorptivity of Titan's Ontario Lacus. *J. Geophys. Res.* 115:E09009
Head IM, Jones DM, Larter SR. 2003. Biological activity in the deep subsurface and the origin of heavy oil. *Nature* 426:344–52
Hofgartner JD, Hayes AG, Lunine JI, Zebker H, Lorenz RD, et al. 2016. Titan's "*Magic Islands*": transient features in a hydrocarbon sea. *Icarus* 271:338–49
Hofgartner JD, Hayes AG, Lunine JI, Zebker H, Stiles BW, et al. 2014. Transient features in a Titan sea. *Nat. Geosci.* 7:493–96
Hofgartner JD, Lunine JI. 2013. Does ice float in Titan's lakes and seas? *Icarus* 223:628–31
Holmes GW, Hopkins DM, Foster HL. 1968. *Pingos in central Alaska*. USGS Bull. 1241-H, US Dep. Inter., Washington, DC
Hörst SM, Vuitton V, Yelle RV. 2008. Origin of oxygen species in Titan's atmosphere. *J. Geophys. Res.* 113:E10006
Howard AD. 1990. Role of hypsometry and planform in basin hydrologic response. *Hydrol. Process.* 4:373–85
Hunten DM. 1973. Escape of H_2 from Titan. *J. Atmos. Sci.* 30:726–32
Iess L, Jacobson RA, Ducci M, Stevenson DJ, Lunine JI, et al. 2012. The tides of Titan. *Science* 337:457–59
Jackson MPA, Vendeville BC, Schultz-Ela DD. 1994. Structural dynamics of salt systems. *Annu. Rev. Earth Planet. Sci.* 22:93–117
Kraal ER, Asphaug E, Moore JM, Lorenz RD. 2006. Quantitative geomorphic modeling of Martian bedrock shorelines. *J. Geophys. Res.* 111:E03001
Kuiper GP. 1944. Titan: a satellite with an atmosphere. *Astrophys. J.* 100:378–83
Le Gall A, Malaska MJ, Lorenz RD, Janssen MA, Tokano T, et al. 2016. Composition, seasonal change and bathymetry of Ligeia Mare, Titan, derived from its microwave thermal emission. *J. Geophys. Res. Planets*. 121:233–51
Lindal GF, Wood GE, Hotz HB, Sweetnam DN, Eshleman VR, Tyler GL. 1983. The atmosphere of Titan: an analysis of the Voyager 1 radio occultation measurements. *Icarus* 53:348–63
Lora JM, Lunine JI, Russell JL, Hayes AG. 2014. Simulations of Titan's paleoclimate. *Icarus* 243:264–73
Lorenz RD. 1994. Crater lakes on Titan: rings, horseshoes and bullseyes. *Planet. Space Sci.* 42:1–4
Lorenz RD. 1996. Pillow lava on Titan: expectations and constraints on cryovolcanic processes. *Planet. Space Sci.* 44:1021–28
Lorenz RD. 1997. Impacts and cratering on Titan: a pre-Cassini view. *Planet. Space Sci.* 45:1009–19
Lorenz RD. 2009. Titan mission studies—a historical review. *JBIS* 62:162–74
Lorenz RD. 2014. Oceanography on Saturn's moon, Titan. *Sea Technology Magazine*, June. **http://www.sea-technology.com/features/2014/0614/5.php**
Lorenz RD. 2015. Voyage across Ligeia Mare: mechanics of sailing on the hydrocarbon seas of Saturn's moon, Titan. *Ocean Eng.* 104:119–28
Lorenz RD, Biolluz G, Encrenaz P, Janssen MA, West RD, Muhleman DO. 2003. Cassini RADAR: prospects for Titan surface investigations using the microwave radiometer. *Planet. Space Sci.* 51:353–64
Lorenz RD, Hayes AG. 2012. The growth of wind-waves in Titan's hydrocarbon seas. *Icarus* 219:468–75
Lorenz RD, Jackson B, Hayes A. 2010a. Racetrack and Bonnie Claire: southwestern US playa lakes as analogs for Ontario Lacus, Titan. *Planet. Space Sci.* 58:724–31
Lorenz RD, Kirk RL, Hayes AG, Anderson YZ, Lunine JI, et al. 2014. A radar map of Titan seas: tidal dissipation and ocean mixing through the throat of Kraken. *Icarus* 237:9–15
Lorenz RD, Lunine JI. 1996. Erosion on Titan: past and present. *Icarus* 122:79–91
Lorenz RD, Lunine JI. 1997. Titan's surface reviewed: the nature of bright and dark terrain. *Planet. Space Sci.* 45:981–92
Lorenz RD, Mitchell KL, Kirk RL, Hayes AG, Aharonson O, et al. 2008. Titan's inventory of organic surface materials. *Geophys. Res. Lett.* 35:L02206

Lorenz RD, Newman C, Lunine JI. 2010b. Threshold of wave generation on Titan's lakes and seas: effect of viscosity and implications for Cassini observations. *Icarus* 207:932–37
Lorenz RD, Oleson S, Woytach J, Jones R, Colazza A, et al. 2015. Titan submarine: vehicle design and operations concept for the exploration of the hydrocarbon seas of Saturn's giant moon. *Lunar Planet. Sci. Conf. Abstr.* 46:1259
Lorenz RD, Wall S, Radebaugh J, Boubin G, Reffet E, et al. 2006. The sand seas of Titan: Cassini RADAR observations of longitudinal dunes. *Science* 312:724–27
Lucas A, Aharonson O, Deledalle C, Hayes AG, Kirk R, Howington-Kraus E. 2014. Insights into Titan's geology and hydrology based on enhanced image processing of Cassini RADAR data. *J. Geophys. Res. Planets* 119:2149–66
Lunine JI. 2009. Saturn's Titan: a strict test for life's cosmic ubiquity. *Proc. Am. Philos. Soc.* 153:403–18
Lunine JI. 2010. Titan and habitable planets around M-dwarfs. *Faraday Discuss.* 147:405–18
Lunine JI, Atreya SK. 2008. The methane cycle on Titan. *Nat. Geosci.* 1:159–64
Lunine JI, Stevenson DJ, Yung YL. 1983. Ethane ocean on Titan. *Science* 222:1229–30
Luspay-Kuti A, Chevrier VF, Cordier D, Rivera-Valentin EG, Singh S, et al. 2015. Experimental constraints on the composition and dynamics of Titan's polar lakes. *Earth Planet. Sci. Lett.* 410:75–83
MacKenzie SM, Barnes JW, Sotin C, Soderblom JM, Le Mouelic S, et al. 2014. Evidence of Titan's climate history from evaporite distribution. *Icarus* 243:191–207
Malaska MJ, Hodyss R. 2014. Dissolution of benzene, naphthalene, and biphenyl in a simulated Titan lake. *Icarus* 242:74–81
Mastrogiuseppe M, Hayes AG, Poggiali V, Seu R, Lunine J, Hofgartner JD. 2016a. Bathymetry and composition of Titan's Ontario Lacus derived from Monte Carlo-based waveform inversion of Cassini RADAR altimetry data. *Icarus*. Submitted
Mastrogiuseppe M, Hayes AG, Poggiali V, Seu R, Lunine J, Hofgartner JD. 2016b. Radar sounding using the Cassini altimeter: waveform modeling and Monte Carlo approach for data inversion of observations of Titan's seas. *IEEE Trans. Geosci. Remote Sens.* In press
Mastrogiuseppe M, Poggiali V, Hayes A, Lorenz R, Lunine J, et al. 2014. The bathymetry of a Titan sea. *Geophys. Res. Lett.* 41:1432–37
McDonald CP, Rover JA, Stets EG, Striegl RG. 2012. The regional abundance and size distribution of lakes and reservoirs in the United States and implications for estimates of global lake extent. *Limnol. Oceanogr.* 57:597–606
McKay CP, Pollack JB, Lunine JI, Courtin R. 1993. Coupled atmosphere-ocean models of Titan's past. *Icarus* 102:88–98
McKay CP, Porco CC, Altheide T, Davis WL, Kral TA. 2008. The possible origin and persistence of life on Enceladus and detection of biomarkers in the plume. *Astrobiology* 8:909–19
McKay CP, Smith HD. 2005. Possibilities for methanogenic life in liquid methane on the surface of Titan. *Icarus* 178:274–76
Michaelides RJ, Hayes AG, Mastrogiuseppe M, Zebker HA, Farr TG, et al. 2016. Constraining the physical properties of Titan's empty lake basins using nadir and off-nadir Cassini RADAR backscatter. *Icarus* 270:57–66
Mitchell KL, Barmatz MB, Jamieson CS, Lorenz RD, Lunine JI. 2015. Laboratory measurements of cryogenic liquid alkane microwave absorptivity and implications for the composition of Ligeia Mare, Titan. *Geophys. Res. Lett.* 42:1340–45
Mitri G, Coustenis A, Fanchini G, Hayes AG, Iess L, et al. 2014. The exploration of Titan with an orbiter and a lake probe. *Planet. Space Sci.* 104:78–92
Moore JM, Howard AD. 2011. Are the basins of Titan's Hotei Regio and Tui Regio sites of former low latitude seas? *Geophys. Res. Lett.* 38:L04201
Moore JM, Howard AD, Morgan AM. 2014. The landscape of Titan as witness to its climate evolution. *J. Geophys. Res. Planets* 119:2060–77
Moriconi ML, Lunine JI, Adriani A, D'Aversa E, Negrao A, et al. 2010. Characterization of Titan's Ontario Lacus region from Cassini/VIMS observations. *Icarus* 210:823–31
Mousis O, Choukroun M, Lunine JI, Sotin C. 2014. Equilibrium composition between liquid and clathrate reservoirs on Titan. *Icarus* 239:39–45

NASA. 2014. *2014 NASA Science Plan*. Washington, DC: NASA
Niemann HB, Atreya SK, Demick JE, Gautier D, Haberman JA, et al. 2010. Composition of Titan's lower atmosphere and simple surface volatiles as measured by the Cassini-Huygens probe gas chromatograph mass spectrometer experiment. *J. Geophys. Res.* 115:E12006
Notarnicola C, Ventura B, Casarano D, Posa F. 2009. Cassini radar data: estimation of Titan's lake features by means of a Bayesian inversion algorithm. *IEEE Trans. Geosci. Remote Sens.* 47:1501–11
NRC (Natl. Res. Counc.). 2011. *Vision and Voyages for Planetary Science in the Decade 2013–2022*. Washington, DC: Natl. Acad. Press
Owen T, Niemann HB. 2009. The origin of Titan's atmosphere: some recent advances. *Philos. Trans. R. Soc. A* 367:607–15
Paillou P, Lunine J, Ruffie G, Encrenaz P, Wall S, et al. 2008a. Microwave dielectric constant of Titan-relevant materials. *Geophys. Res. Lett.* 35:L18202
Paillou P, Mitchell K, Wall S, Ruffie G, Wood C, et al. 2008b. Microwave dielectric constant of liquid hydrocarbons: application to the depth estimation of Titan's lakes. *Geophys. Res. Lett.* 35:L05202
Perron JT, Lamb MP, Koven CD, Fung IY, Yager E, Adamkovics M. 2006. Valley formation and methane precipitation rates on Titan. *J. Geophys. Res.* 111:E11001
Picardi G, Seu R, Coradini A, Zampolini E, Ciaffone A. 1992a. Radar geomorphologic characterization of Titan. *Proc. Radar 92 Int. Conf.*, *Oct. 12–13*, *Brighton*, *UK*, pp. 254–57. London: Inst. Electr. Eng.
Picardi G, Seu R, Coradini A, Zampolini E, Ciaffone A. 1992b. The radar system for the exploration of Titan. *Nuovo Cim. C* 15:1149–61
Porco CC, West RA, Squyres S, McEwen A, Thomas P, et al. 2004. Cassini imaging science: instrument characteristics and anticipated scientific investigations at Saturn. *Space Sci. Rev.* 115:363–497
Pross A, Pascal R. 2013. The origin of life: what we know, what we can know and what we will never know. *Open Biol.* 3:120190
Raulin F, Brasse C, Poch O, Coll P. 2012. Prebiotic-like chemistry on Titan. *Chem. Soc. Rev.* 41:5380–93
Raulin F, McKay C, Lunine J, Owen T. 2009. Titan's astrobiology. In *Titan from Cassini-Huygens*, ed. RH Brown, JP Lebreton, JH Waite, pp. 215–33. Dordrecht, Neth.: Springer
Roe HG, Grundy WM. 2012. Buoyancy of ice in the CH_4–N_2 system. *Icarus* 219:733–36
Romanberdiel T, Gapais D, Brun JP. 1995. Analog models of laccolith formation. *J. Struct. Geol.* 17:1337–46
Schneider T, Graves SDB, Schaller EL, Brown ME. 2012. Polar methane accumulation and rainstorms on Titan from simulations of the methane cycle. *Nature* 481:58–61
Schulze-Makuch D, Grinspoon DH. 2005. Biologically enhanced energy and carbon cycling on Titan? *Astrobiology* 5:560–67
Schulze-Makuch D, Grinspoon DH. 2006. Plausible metabolic pathways and energy cycling on Titan. *Origins Life Evol. Biosph.* 36:324–25
Sharma P, Byrne S. 2011. Comparison of Titan's north polar lakes with terrestrial analogs. *Geophys. Res. Lett.* 38:L24203
Sotin C, Barnes JW, Lawrence KJ, Soderblom JM, Audi E, et al. 2015. *Bright, tidal currents between Titan's seas detected by solar glints*. Presented at AGU Fall Meet., Dec. 14–18, San Francisco. Abstr. P12B-04
Srokosz MA, Challenor PG, Zarnecki JC, Green SF. 1992. Waves on Titan. *Proc. Symp. Titan*, *Sept. 9–12 1991*, *Toulouse*, *Fr.*, pp. 321–23. Noordwijk, Neth.: Eur. Space Agency
Stephan K, Jaumann R, Brown RH, Soderblom JM, Soderblom LA, et al. 2010. Specular reflection on Titan: liquids in Kraken Mare. *Geophys. Res. Lett.* 37:L07104
Stofan ER, Elachi C, Lunine JI, Lorenz RD, Stiles B, et al. 2007. The lakes of Titan. *Nature* 445:61–64
Stofan ER, Lorenz R, Lunine J, Bierhaus EB, Clark B, et al. 2013. TiME—the Titan Mare Explorer. *Proc. 2013 IEEE Aerosp. Conf.*, *Mar. 2–9*, *Big Sky*, *Mont.*, pp. 1–10. Piscataway, NJ: IEEE
Strobel DF. 2010. Molecular hydrogen in Titan's atmosphere: implications of the measured tropospheric and thermospheric mole fractions. *Icarus* 208:878–86
Tan SP, Kargel JS, Jennings DE, Mastrogiuseppe M, Adidharma H, Marion GM. 2015. Titan's liquids: exotic behavior and its implications on global fluid circulation. *Icarus* 250:64–75
Tan SP, Kargel JS, Marion GM. 2013. Titan's atmosphere and surface liquid: new calculation using Statistical Associating Fluid Theory. *Icarus* 222:53–72

Thompson WR, Squyres SW. 1990. Titan and other icy satellites: dielectric properties of constituent materials and implications for radar sounding. *Icarus* 86:336–54
Tobie G, Lunine JI, Monteux J, Mousis O, Nimmo F. 2014. The origin and evolution of Titan. In *Titan: Interior, Surface, Atmosphere, and Space Environment*, ed. I Müller-Wodarg, CA Griffith, E Lellouch, TE Cravens, pp. 29–62. Cambridge, UK: Cambridge Univ. Press
Tokano T. 2005a. Meteorological assessment of the surface temperatures on Titan: constraints on the surface type. *Icarus* 173:222–42
Tokano T. 2005b. Thermal structure of putative hydrocarbon lakes on Titan. *Adv. Space Res.* 36:286–94
Tokano T. 2009a. Impact of seas/lakes on polar meteorology of Titan: simulation by a coupled GCM-Sea model. *Icarus* 204:619–36
Tokano T. 2009b. Limnological structure of Titan's hydrocarbon lakes and its astrobiological implication. *Astrobiology* 9:147–64
Tokano T. 2010. Simulation of tides in hydrocarbon lakes on Saturn's moon Titan. *Ocean Dyn.* 60:803–17
Tokano T, Lorenz RD. 2015. Wind-driven circulation in Titan's seas. *J. Geophys. Res. Planets* 120:20–33
Tung SH, Lee HY, Raghavan SR. 2008. A facile route for creating "reverse" vesicles: insights into "reverse" self-assembly in organic liquids. *J. Am. Chem. Soc.* 130:8813–17
Turtle EP, Perry JE, Hayes AG, Lorenz RD, Barnes JW, et al. 2011a. Rapid and extensive surface changes near Titan's equator: evidence of April showers. *Science* 331:1414
Turtle EP, Perry JE, Hayes AG, McEwen AS. 2011b. Shoreline retreat at Titan's Ontario Lacus and Arrakis Planitia from Cassini Imaging Science Subsystem observations. *Icarus* 212:957–59
Turtle EP, Perry JE, McEwen AS, DelGenio AD, Barbara J, et al. 2009. Cassini imaging of Titan's high-latitude lakes, clouds, and south-polar surface changes. *Geophys. Res. Lett.* 36:L02204
Vixie G, Barnes JW, Jackson B, Rodriguez S, Le Mouélic S, et al. 2015. Possible temperate lakes on Titan. *Icarus* 257:313–23
Wall S, Hayes A, Bristow C, Lorenz R, Stofan E, et al. 2010. Active shoreline of Ontario Lacus, Titan: a morphological study of the lake and its surroundings. *Geophys. Res. Lett.* 37:L05202
Williams PW. 2008. The role of the epikarst in karst and cave hydrogeology: a review. *Int. J. Speleol.* 37:1–10
Wood CA. 2015. North polar crater and lake basins: a variety of shapes—a single origin? *Lunar Planet. Sci. Conf. Abstr.* 46:2490
Wood CA, Mitchell KL, Lopes RMC, Radebaugh J, Stoffan E, Lunine J. 2007. Volcanic calderas in the north polar region of Titan. *Lunar Planet. Sci. Conf. Abstr.* 46:1454
Wye LC, Zebker HA, Lorenz RD. 2009. Smoothness of Titan's Ontario Lacus: constraints from Cassini RADAR specular reflection data. *Geophys. Res. Lett.* 36:L16201
Zebker H, Hayes A, Janssen M, Le Gall A, Lorenz R, Wye L. 2014. Surface of Ligeia Mare, Titan, from Cassini altimeter and radiometer analysis. *Geophys. Res. Lett.* 41:308–13

Annual Review
of Earth and
Planetary Sciences
Volume 44, 2016

Contents

Tektites, Apollo, the Crust, and Planets: A Life with Trace Elements
Stuart Ross Taylor 1

Environmental Detection of Clandestine Nuclear Weapon Programs
R. Scott Kemp 17

From Tunguska to Chelyabinsk via Jupiter
Natalia A. Artemieva and Valery V. Shuvalov 37

The Lakes and Seas of Titan
Alexander G. Hayes 57

Inference of Climate Sensitivity from Analysis of Earth's Energy Budget
Piers M. Forster 85

Ocean Basin Evolution and Global-Scale Plate Reorganization Events Since Pangea Breakup
R. Dietmar Müller, Maria Seton, Sabin Zahirovic, Simon E. Williams, Kara J. Matthews, Nicky M. Wright, Grace E. Shephard, Kayla T. Maloney, Nicholas Barnett-Moore, Maral Hosseinpour, Dan J. Bower, and John Cannon 107

Lithification Mechanisms for Planetary Regoliths: The Glue that Binds
John G. Spray 139

Forensic Stable Isotope Biogeochemistry
Thure E. Cerling, Janet E. Barnette, Gabriel J. Bowen, Lesley A. Chesson, James R. Ehleringer, Christopher H. Remien, Patrick Shea, Brett J. Tipple, and Jason B. West 175

Reconstructing Ocean pH with Boron Isotopes in Foraminifera
Gavin L. Foster and James W.B. Rae 207

Sun, Ocean, Nuclear Bombs, and Fossil Fuels: Radiocarbon Variations and Implications for High-Resolution Dating
Koushik Dutta 239

Climate Sensitivity in the Geologic Past
Dana L. Royer 277

Redox Effects on Organic Matter Storage in Coastal Sediments During the Holocene: A Biomarker/Proxy Perspective
Thomas S. Bianchi, Kathryn M. Schreiner, Richard W. Smith, David J. Burdige, Stella Woodard, and Daniel J. Conley 295

Fracking in Tight Shales: What Is It, What Does It Accomplish, and What Are Its Consequences?
J. Quinn Norris, Donald L. Turcotte, Eldridge M. Moores, Emily E. Brodsky, and John B. Rundle 321

The Climate of Titan
Jonathan L. Mitchell and Juan M. Lora 353

The Climate of Early Mars
Robin D. Wordsworth 381

The Evolution of Brachiopoda
Sandra J. Carlson 409

Permafrost Meta-Omics and Climate Change
Rachel Mackelprang, Scott R. Saleska, Carsten Suhr Jacobsen, Janet K. Jansson, and Neslihan Taş 439

Triple Oxygen Isotopes: Fundamental Relationships and Applications
Huiming Bao, Xiaobin Cao, and Justin A. Hayles 463

Cellular and Molecular Biological Approaches to Interpreting Ancient Biomarkers
Dianne K. Newman, Cajetan Neubauer, Jessica N. Ricci, Chia-Hung Wu, and Ann Pearson 493

Body Size Evolution Across the Geozoic
Felisa A. Smith, Jonathan L. Payne, Noel A. Heim, Meghan A. Balk, Seth Finnegan, Michał Kowalewski, S. Kathleen Lyons, Craig R. McClain, Daniel W. McShea, Philip M. Novack-Gottshall, Paula Spaeth Anich, and Steve C. Wang 523

Nuclear Forensic Science: Analysis of Nuclear Material Out of Regulatory Control
Michael J. Kristo, Amy M. Gaffney, Naomi Marks, Kim Knight, William S. Cassata, and Ian D. Hutcheon 555

Biomarker Records Associated with Mass Extinction Events
Jessica H. Whiteside and Kliti Grice 581

Impacts of Climate Change on the Collapse of Lowland Maya Civilization
Peter M.J. Douglas, Arthur A. Demarest, Mark Brenner, and Marcello A. Canuto ... 613

Evolution of Oxygenic Photosynthesis
Woodward W. Fischer, James Hemp, and Jena E. Johnson 647

Crustal Decoupling in Collisional Orogenesis: Examples from the East Greenland Caledonides and Himalaya
K.V. Hodges 685

Mass Fractionation Laws, Mass-Independent Effects, and Isotopic Anomalies
Nicolas Dauphas and Edwin A. Schauble 709

Indexes

Cumulative Index of Contributing Authors, Volumes 35–44 785

Cumulative Index of Article Titles, Volumes 35–44 790

Errata

An online log of corrections to *Annual Review of Earth and Planetary Sciences* articles may be found at http://www.annualreviews.org/errata/earth